ASSESSING AGRICULTURAL DROUGHT IMPACT ON SOIL SALINITY IN BUA YAI AND SIDA DISTRICTS, NAKHON - RATCHASIMA PROVINCE, THAILAND

YOOTTHAPOOM POTIRACHA

February, 2017

SUPERVISORS:
Assist. Prof. Dr. D.B.P. Shrestha
Assist. Prof. Dr.Ir. J. Ettema
Assist. Prof. Dr. C. Lievens

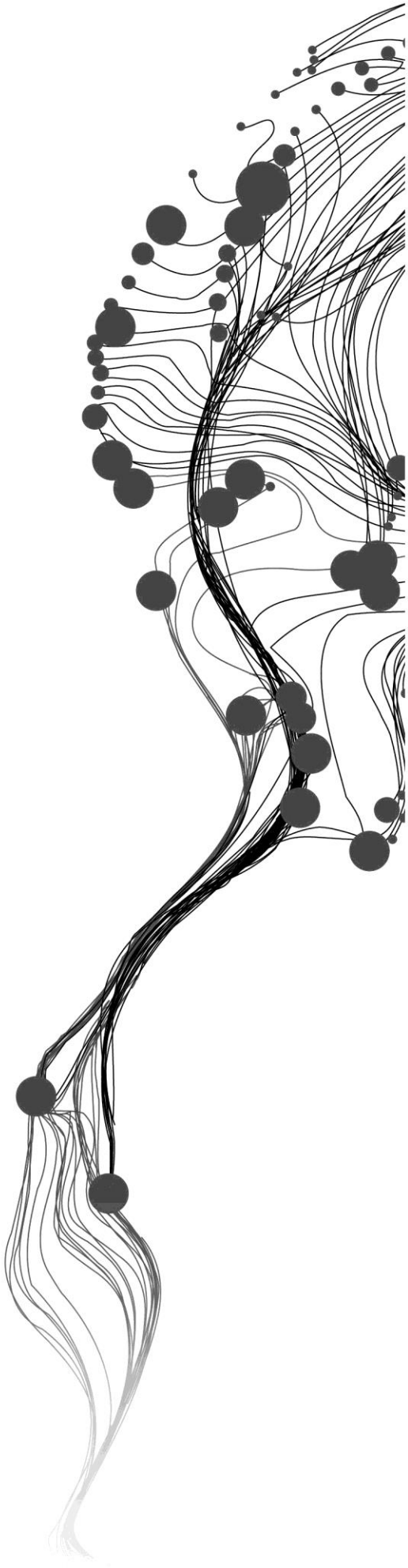

ASSESSING AGRICULTURAL DROUGHT IMPACT ON SOIL SALINITY IN BUA YAI AND SIDA DISTRICTS, NAKHON -RATCHASIMA PROVINCE, THAILAND

YOOTTHAPOOM POTIRACHA

Enschede, The Netherlands, February, 2017

Thesis submitted to the Faculty of Geo-Information Science and Earth Observation of the University of Twente in partial fulfilment of the requirements for the degree of Master of Science in Geo-information Science and Earth Observation.
Specialization: Applied Earth Sciences, with specialization in Natural Hazards, Risk and Engineering

SUPERVISORS:
Assist. Prof. Dr. D. B. P. Shrestha
Assist. Prof. Dr.Ir. J. Ettema
Assist. Prof. Dr. C. Lievens

THESIS ASSESSMENT BOARD:
Prof. Dr. V. Jetten (Chair)
Assoc. Prof. Dr.Ir. T. Bogaard (External Examiner, TU Delft)

ABSTRACT

Soil salinity is often found in arid areas as a result of a complex salinity process of many factors at particular locations. Landscape, climate and human activities are the most important factors which influence on salinity levels and processes. Salinity problem usually becomes a problem of land development when the concentration of salt adversely impacts plant growth. Bua Yai and Sida districts in Nakhonratchasima province in Thailand are the highly susceptible areas to reoccurring soil salinity due to underlying salt beds, drought conditions and the strengthening effect of hydrologic mechanisms. Rice paddy cultivation is the major activity of local people in this area that strongly depends on water supply. Therefore, drought is the critical factor for soil salinity of rice production in those districts. Soil salinity assessment for agricultural drought and its impacts is the important application but there are no applications, which accounts for soil salinity in agricultural areas.

This research mainly focuses on enhancing the understanding and applying of the basic concepts of agricultural drought for soil salinity assessment. A case study of the pilot area in northeast of Thailand provides an example of the effect of drought and soil salinity in 2016 as compared to other years. Three main methodological approaches, which are salinity proxies' correlations, spatial modelling for susceptibility assessment, and drought impact determining, were applied in this study. The research has established the relationship between main salinity proxies and electronic conductivity (EC) values to define the rules of a decision tree which were applied in a GIS environment with ILWIS Open 3.8.5.0 for susceptibility mapping. Standardized Precipitation Index (SPI) was used to define drought conditions together with monthly soil moisture (SM) extracted from Radarsat-2 image by using semi-empirical model.

Soil texture, elevation, land use and the Normalized Difference Vegetation Index (NDVI) were considered as the important salinity proxies. All conditional factors were applied in the hierarchy of the decision tree in order to produced susceptibility map. For instance, fine soil textured in lower elevation terrain, which are located in rice paddy/mash and swamp areas with lower NDVI values, was defined as very high soil salinity prone area. The soil salinity susceptibility map in 2016 was classified into 5 classes' none, low, moderate, high and very high which covered areas of 0.93 (18.68%), 2.76 (55.12%), 0.72 (14.30%), 0.45 (9.06%) and 0.14 (2.84%) respectively. For drought situation and salinity impacts in 2016, 3 month standardized precipitation index (SPI) were in the ranges from -1.32 to 0.79, and 6 month SPI in the ranges of -1.04 to 0.83, the interpretation of both the SPI value ranges in 2016 can be interpreted as a normal year (no drought). The SPI results show a good relationship with estimated SM from Radarsat-2 images in 2016 and rice productions during 2011-2015. Estimated SM was validated by SM measurement at the same time of model measurement and exhibited with $R^2 = 0.69$. It is reported that high rice production is obtained in a higher interval of SPI, which is directly related to high SM leading to low soil salinity.

ACKNOWLEDGEMENTS

First of all, I am thankful my family always standing by my side when time gets hard or happy. To studying here, my inspiration comes from mom and dad and giving my success to them.

I am grateful to Dr. D.B.P. Shrestha and Dr. D. Alkema for giving me the opportunity to study in ITC. I even couldn't have started with my ITC life if not for your help. I am highly appreciative to my supervisors for their valuable support, useful comments, critical thinking and encouragement. They impart their expertise and scientific knowledge, taught me how to properly write, and they have been extremely patient understanding and editing my English. Thanks to my supervisor, Dr. Dhruba, for his patience and steady support during the most difficult time and during my field work. I want to extend my appreciation to my second supervisors, Dr. Ir. J. Ettema and Dr. C. Lievens for very clear guidance and good intension.

I would like to thank the Royal Thai Government Scholarships for providing this opportunity of a lifetime. I would like to thank Ruamporn Moonchan and the Thai Land Development Department for assisting during the fieldwork. I also would like to thank my office, GISTDA, for allowing me to pursue further studies abroad.

I thank my MSc friends especially my AES family for adding color and dimension to my ITC life. I would like to thank my Thai friends in Enschede, especially Nattapon Khammad my super brother, for all the experiences we have share together, especially for cooking. Special thanks to Beverly Brebante and Retch Oneko Grachen for their friendship, which I will always treasure.

I dedicate this to my parents for their unconditional love and support. I couldn't have done this thesis if without your guidance and love.

And finally, I thank the Thai people, especially to King Rama-IX. May we always live in peace and prosperity.

TABLE OF CONTENTS

LIST OF FIGURES

LIST OF TABLES

1. INTRODUCTION

1.1. Background

Drought is a silent disaster with a variety of impact, from the community grassroots to the national levels. It particularly affects agriculture resulting into serious economic loss and various social problems (Sánchez, 2008). Drought is defined as water deficit from a simple regulation of the hydrological cycle (Sheffield & Wood, 2011). Specifically, Senaut (2015) described it as the decrease in amount of rainfall, runoff and soil moisture for a time period compared to the climatology in each region. Based on the severity-area-duration (SAD) analysis, Asia had the highest frequency of extensive drought events in the World from 1986 to 2003 (Sheffield & Wood, 2011).

In the scientific aspect, drought is generally classified into four main types: meteorological drought, agricultural drought, hydrological drought and socio-economic drought (Sánchez, 2008; Sheffield & Wood, 2011; Senaut, 2015). The classification is based on the following elements: (1) space, time as month, season or year, (2) meteorology in terms of intensity of temperature, (3) precipitation in specific period of time and space and (4) hydrology which refers to runoff volume, average ground water level, and average soil moisture (Sánchez, 2008). All types of drought are associated with the physical parameters of meteorology (Wilhite & Glantz, 1985a) and climate fluctuations such as temperature anomalies and extreme weak precipitation caused by El Niño phenomenon (FAO, 2014).

This study will focus on the agricultural drought which is considered as soil water deficiency under natural climate variability that affects plant water stress and reduces biomass and crop yield (The US National Drought Mitigation Center, 2016). The effect can be attributed to precipitation shortage, decreased groundwater, increased evapotranspiration and so forth to relate with meteorological drought (Wilhite et al., 1985b; Zargar et al., 2011). In 1986 to 2010, agricultural drought due to El Niño affected the crop season in Asia, including Thailand (FAO, 2014). The drought crisis in the country has been occurring almost every year including the dry season of 2016. Based on literature, intensification of drought is attributed to reduction of accumulated rainfall per year (Thaiturapaisan, 2016) and rise of extreme temperature (IPCC, 2012). RID (2015) and Thaiturapaisan (2016) presented the view that the rainfall anomaly between 2014 and 2015 affected the accumulation of annual rainfall causing the dip that was below the 30-years average (1981-2010) and greatly influenced the depletion of water supply in 2016. In addition, the breaking of maximum temperature in many provinces of Thailand were recorded with the maximum temperature in 2015 being 43.1 °C (Thai Meteorological Department, 2015). These factors have resulted to extreme effects that were highly reflected as long-lasting consequences to the society, ecosystems and natural environment (IPCC, 2012). Attempts to mitigate such impacts has had research look into drought parameters.

Drought forecasting is an important component of drought modeling and has been useful risk management by using drought indices as a tool for assessing drought severity in spatial and temporal conditions (Mishra & Singh, 2011). The forecast system has been developed from the aggregation of descriptive model based on historical information with monitoring system to observe current hydro-meteorological variables (Sánchez, 2008). To assess the severity, duration and spatial extent of drought, drought indices have been applied. Owing to complexity of these conditions, remote sensing (RS) and geographic information system (GIS) techniques are applicable manner to model drought scenarios with

indices and in situ data for risk assessment and hazard visualization in a small spatial and temporal extent (Belal, El-Ramady, Mohamed, & Saleh, 2014). In particular, RS provides information and datasets with high spatial resolution to regional drought monitoring and fill the gap of information in drought prone areas without ground measurement networks that help to make decision on drought activities and related policies (Wardlow, Anderson, & Verdin, 2012).

Drought indices determine the severity of meteorological and agricultural droughts from analysis of time series rainfall data (Heim, 2002; Naresh Kumar, et al., 2015). National Weather Service (2016) defines a drought index as computed value which refer to some of the cumulative effects from a prolonged and abnormal moisture deficiency. The utilization of drought indices can be beneficial for subsistent farming specifically rainfed paddy cultivation fields in a non-irrigation zone (Jeong et al., 2014). In Thailand, drought crisis often occur during dry season (February to May), which has significant impacts on crop cycle and productions (Mapraneat, 2014; Thaiturapaisan, 2016). For this research, drought indices based on remotely sensed parameters were applied for agricultural drought monitoring. NDVI as drought index is often used to characterize vegetation stages based on the water supply condition (Dunkel, 2009). Moreover drought indices were developed from the meteorological variables and are widely used to determine the drought situation in a global scale (Dunkel, 2009). Among these indices are the Palmer Drought Severity Index (PDSI), and Standardized Precipitation Index (SPI). The PDSI method uses precipitation, temperature and soil moisture data to classify levels of agricultural drought and identify drought abnormality in regional or national scales (Belal et al., 2014). For SPI index, the values are calculated from historical rainfall data to monitor meteorological drought (Hao & AghaKouchak, 2013) and provide drought early warning and risk management (Belal et al., 2014). The SPI calculations are based on long term rainfall data, and have been a popular meteorological index. It has been utilized for assessing drought severity and its impacts to water resources (Zargar et al., 2011).

Soil moisture (SM) is an important soil property to determine water crisis in relation to agricultural drought. SM estimations are mostly accurate when measured directly from the ground; but this technique is time consuming, costly and only provides data in a specific coverage. Alternatively, advance remote sensing can be useful to monitor SM at lower cost and shorter time with high temporal and spatial resolutions. The retrieval of SM has been estimated from direct and indirect ways in remote sensing (RS) approach such as optical, thermal infrared (TIR) and active and passive microwave (Wang & Qu, 2009). Microwave sensors are directly considered to characterize near surface moisture in bare soil and low vegetation with less effect from atmospheric conditions (Moran et al., 2004). Limitations to active remote sensed soil moisture have include wavelength, polarization and incidence angle (Shi et al., 2012), which affect the accuracy of SM estimation (Brisco et al., 2008). Despite this, the SM can be retrieved by many RS techniques like multi-angle TIR, Synthetic aperture radars (SAR) change detection and SAR data fusion (Moran et al., 2004). Since RADARSAT-2 was operated in December of 2007, several approaches of SM models that integrate SAR backscatter and local conditions have been taken for estimating surface soil moisture such as simple empirical models, semi-empirical models and physically-based models (Mcnairn et al., 2010). Agriculture and Agri-Food Canada (AAFC) has been evaluated the accuracy and monitored SM temporal distribution, so SAR is suitable for estimating near surface soil moisture for an agriculture sectors (Mcnairn et al., 2010; McNairn et al., 2012).

Soil salinity, one of the prominent land degradation problems often coincides with agricultural drought and is observed during the dry season (Quantin et al., 2008). Currently, salinity problems have been increasing particularly in arid and semi-arid regions of North America, South Africa, Australia, China, Argentina, Egypt, India, Iran, Pakistan and Thailand (Ghassemi et al., 1995). In Thailand, salt-affected areas are about 3.58 million hectares wherein 3 million hectares are inland soil and the remaining 0.58 million hectares are coastal saline soils (Shahid, 2013). The increasing trend of this problem have been

attributed to some factors such as climate, soil, vegetation and land use (Morgan & Jankowski, 2004). Previous studies show that soil salinity is significantly correlated with soil moisture, rainfall (Haron & Dragovich, 2010) and land surface temperature (LST)(Wu et al., 2014).

Similarly, irrigation system can also be a contributing factor in the salinization of soil. Canal leakage may contribute to the seepage into an area that increases and disturbs the saline groundwater by emerging on the surface causing salinity (Wannakomol, 2005). Saline patches appear on soil surface during the dry period when the highest intensity of salinity in shallow groundwater occurs. A degree of soil salinization is the result of an interaction between rising groundwater level due to capillary rise effect and artesian pressure flow system (Abdolrahim, 2003; Quantin et al., 2008). Natural concentration of salt in the soil wherein as shallow saline groundwater rise to the soil surface, evaporation occurs and surface soil salinity results (Wannakomol, 2005; Clermont-Dauphin et al., 2010). Soil salinization is also aggravated by deforestation and poor irrigation and cultivation which accelerates salt dissolution and transfer through surface. In the upland areas of northeast Thailand, land degradation is attributed to land clearing for expansion of crop cultivation like cassava, sugarcane and kenaf. Under natural vegetation conditions, water use and evapotranspiration are high, while groundwater use and transpiration are low under deforestation conditions (Loffler et al., 1984). The latter contributes to the increase in infiltration and groundwater recharge. The shallow roots allow water to penetrate to the salt bed layers which is part of the Maha Sarakham Formation underlying the northeast of Thailand. This results in saline seepage on lower slopes and valley (Land development department, 2009). Rock salt in the Maha Sarakham Formation composed of claystone, siltstone, and three rock salt beds are the main sources of soil and groundwater salinization in the Khorat Plateau (Department of Mineral Resources, 1999).

Salinity is one of the factors that causes crop failure effect to crop yield and productivity in global scale (Baghalianb et al., 2008). Each crop has a different level of salinity tolerance (Ayers & Westcot, 1985). When soil salinity increases, crop yield will decrease as an inverse correlation (Warrence, Bauder, & Pearson, 2003). Based on the study of Hall et al. (2004), revenue in Kalasin and Nakhon Ratchasima province in the last 30 years fell 484.14 baht per rai (0.675 km2) per year wherein total revenue lost in the northeast amounted to about 2,518 million baht (63 million euro) per year and was attributed to soil salinity.

Limited knowledge on salinity processes is a major concern as this will have an effect on the conventional agriculture practices in the area. Crop cycles should take into account the present soil salinity conditions of an area in order to address the crop growth and crop yield issues as carried out in the research work of Lacerda et al. (2011).

1.2. Research Problem

A third of northeastern Thailand's total land area is covered with saline soil, mainly located on the agricultural lands. This has resulted to lowered crop production, and ultimately results to economic and societal problems. Soil salinity is a land degradation problem in the area which is intensified during dry season. The spatial distribution of saline soils depends on the characteristics of soil properties and groundwater level (Seeboonruang, 2013). However, there are also some factors which enhance the salinization process. Removal of natural vegetation particularly upstream due to agricultural land expansion has contributed to the rise of saline groundwater in the valley resulting in the increase of salt deposits at the surface. When natural vegetation is replaced by cultivated crop, the deep root system is replaced by a shallow root system that causes groundwater rising and can be more uptake through soil surface with capillary action during dry season. These factors have an impact on the salinity processes.

To understand the occurrences of salinity at the surface as well as the spatial distribution, it is necessary to identify the processes involved in its formation, as well as the degree of salinization, in the area in order to efficiently address the problem.

1.3. Objectives and research questions

The main objective of this study is to establish the relationship between drought conditions and soil salinity progress in time and space within crop cycle and stages in Kut Chok and Non Pradu sub-districts by using soil moisture, precipitation and vegetation indices obtained from remotely sensed data.

The specific objectives are:

- To establish salinity proxies using local information of vegetation types, elevation, soil properties and soil moisture state to soil salinity
- To develop a spatial model predicting soil salinity based on vegetation types, elevation, soil properties and soil moisture state to soil salinity
- To determine the impact of drought on soil salinity and crop growth using remotely sensed data by means of several drought indices and salinity proxies

The research questions are:

- How is (degree of) salinity illustrated/exemplified in vegetation types, elevation, soil properties and soil moisture?
- Does the spatial model represent the soil salinity scenario of the study area?
- What is the extent of salinity distribution in different season?
- Does soil moisture generated from Synthetic aperture radars (SAR) image coincide with the ground truth data?
- How can drought index be used to soil salinity conditions in the area?
- How soil salinity affects the crop stage and production?

2. MATERIALS AND METHODS

2.1. Study area

2.1.1. Location and Territory

The study area (Figure 2.1) is located in a commune region of Bua Yai and Sida districts in Nakhon Ratchasima province (Korat) in the northeastern part of Thailand extending 15°32'28" to 15°34'8" latitude to 102°28'5" to 102°30'4" longitude. It covers approximately 5 km² surface area at a distance of 100 km from a Korat city.

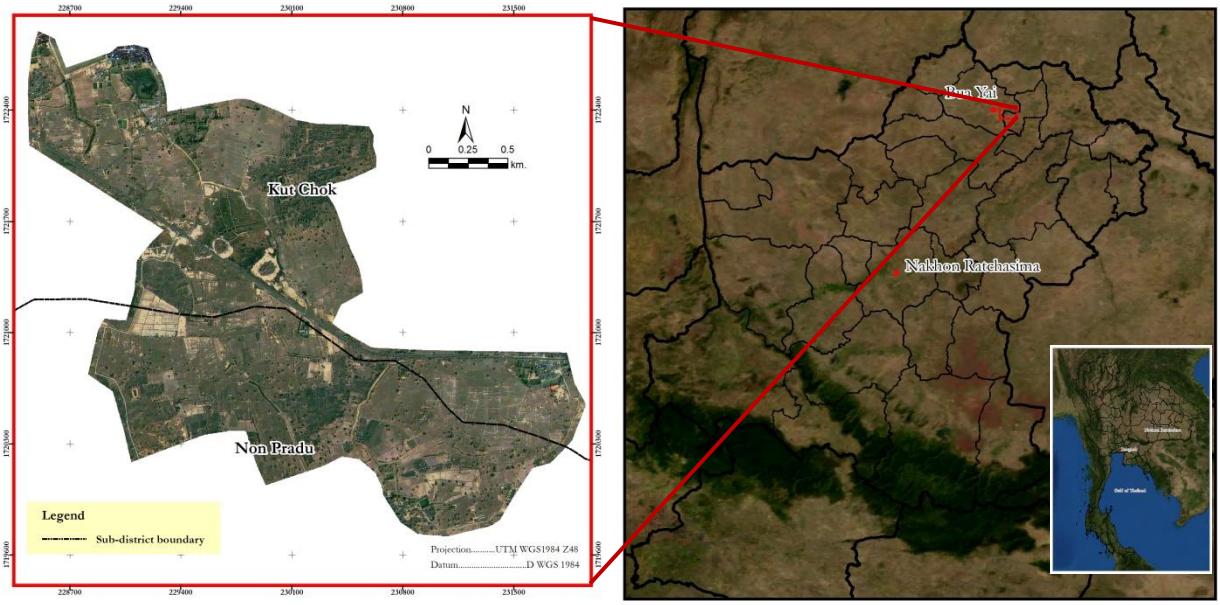

Figure 2-1: Location of the study area in Bua Yai and Sida districts in Nakhon Ratchasima province of northeast. Thailand.

2.1.2. Climate

Climate of the study area is classified as tropical monsoon, which can be divided into 3 seasons: rainy, winter and summer. Average annual precipitation, temperature and relative humidity are 1023 mm, 27.1 °C and 70.0% respectively (Table 2-1). Rainy season starts from May to October from the influence of the southwest monsoon. As a result, the climate is moist and rainy. September has the maximum precipitation of 222 mm and the maximum average relative humidity of 80%. Winter season starts from November to February from the influence of the northeast monsoon, which sweeps cold and drought. December has the lowest temperature (23.3 °C), also precipitation is lowest (3.4 mm). Summer starts from March to April, when the climate is hot and torrid. April has the highest average temperature of 29.8 °C and February and March have the lowest average relative humidity of 61%. The climate statistics from Nakhon Ratchasima meteorological station are used to represent climate in the sub district can be summarized as shown in Table 2-1 ("Thai Meteorological Department," 2016).

Table 2-1: The climate statistics from Nakhon Ratchasima meteorological station during 1986 to 2015 derive from Thai Meteorological Department, 2016.

Month	Rainfall (mm.)	Rainy day	Maximum temperature (°c)	Minimum temperature (°c)	Average temperature (°c)	Relative humidity (%)
January	5.9	0.9	30.9	17.9	24.0	64
February	18.2	2.4	33.5	20.5	26.5	61
March	37.4	5.1	35.7	22.8	28.7	61
April	63.3	7.6	36.6	24.5	29.8	65
May	138.4	13.7	35.1	24.8	28.9	72
June	114.1	13.2	34.3	24.8	28.8	73
July	115.5	13.8	33.8	24.4	28.4	73
August	146.8	13.8	33.2	24.2	28.0	75
September	221.8	16.5	32.2	23.8	27.2	80
October	133.2	18.2	31.0	22.9	26.5	78
November	25.3	11.5	29.9	20.6	25.0	72
December	3.4	3.6	29.2	17.7	23.3	66
Summary	1,023.3	120.3	-	-	-	-
Average	-	-	33.0	22.4	27.1	70.0

2.1.3. Topography, soil and Land use

Topography is characterized mostly by flat to gently rolling landscape with elevation ranging from 158 to 168 m above mean sea level. The area is underlain by, rock salt layer of Cretaceous Maha Sarakham Formation (Department of Mineral Resources, 1999) with an average thickness of 250 m (Gardner et al., 1967). It is composed of a top to bottom sequence of claystone, siltstone, and three rock salt beds which are the main sources of soil and groundwater salinization (Wannakomol, 2005). The catchment area that causes salt diffusion especially in the upper salt zone directly contacts of the soil layer, so salt dome and salt anticline occur in some areas (Warren, 1999; Wannakomol, 2005).

Soil are fine-loamy (52.6%), fine (21%) coarse-loamy (12%) and fine-silty(6.5 %). The available soil type map at 1:4,000 scale from LDD is based on ortho-photo image interpretation and field survey during October 2014 – April 2015. This area (Figure 2-2)

Land use is mainly subsistence agriculture. Crops grown are paddy rice, cassava and sugarcane. Moreover, the study area which is within a non-irrigation zone is generally utilized for subsistent farming with rice cultivation (83.3%), cassava (0.35%) while portion of elevated areas are used for eucalyptus plantations (0.1%). Other land use activities in the areas include fish farming (1.7%), degraded deciduous forest (1.05%), grass (0.7%), scrub (2.5%) swamp (4.3%), water bodies (2%), and settlement area (4%)

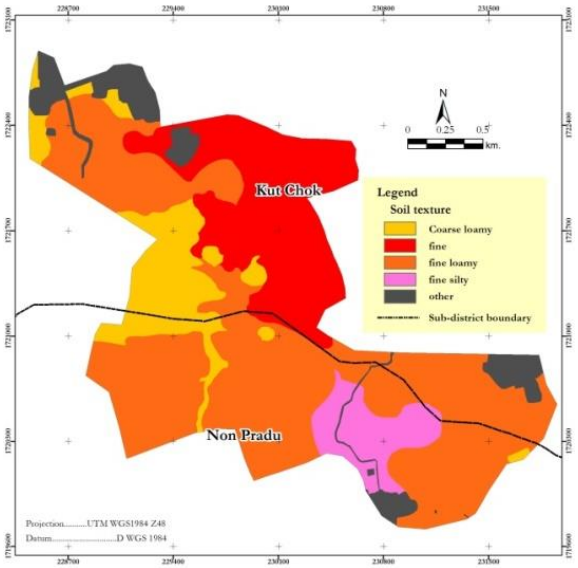

Figure 2-2: 2015 Soil type map was produced by IDD at 1:4,000 scale.

2.2. Materials

2.2.1. Data

Ancillary datasets

The secondary data for climate, vegetation, soil moisture and salinity can be collected from the agencies LDD, TMD, RD, DOAE, DGR and GISTDA, all in digital format. Table 2-2 summarizes these datasets.

Table 2-2: Summary of ancillary datasets collected from secondary sources with details on the data types, period of the dataset retrieval and information on measurement location and/ or horizontal scale.

Type	Data	Year	Details	Source
Climate	Daily rainfall	1986 – 2015	Nakhon Ratchasima, Pak Chong and Chok Chai stations	TMD
		2006 – 2015	Bua Yai and Sida stations	
	Daily relative humidity	1986 – 2015	Nakhon Ratchasima, Pak Chong and Chok Chai stations	
	Daily pan evaporation	1986 – 2015	Nakhon Ratchasima, Pak Chong and Chok Chai stations	
	Daily minimum and maximum temperature	1986 – 2015	Nakhon Ratchasima, Pak Chong and Chok Chai stations	
Soil	Soil unit map	January 2016	scale 1:4,000 in a study area	LDD
	Ksat and bulk density	January 2016	15 points in a lower part of the study area	LDD
	Groundwater level (meter)	January 2016	19 well points in 1 districts	DGR
			15 points of standpipe piezometer	LDD
Vegetation	Land use	2012	Level 3 classification scale 1:50,000	LDD
	Root depth		Root depth of rice in different stages of 3 main genes	RD
	Crop production	2015	Rice production of rice parcel (kg/rai)	LDD
		2010 – 2015	Average main crop production of 2 districts (kg/rai)	DOAE
	PROBA-V	September 2015 – October 2016	10-day NDVI composites 300-meter resolution from	ESA
Elevation	Digital Elevation Model		5 meter resolution	LDD
Soil moisture	Radarsat-2	September 2015 – October 2016	C-band SAR image, ScanSAR mode 30-meter resolution from	GISTDA

Climatic data

Climatic data were obtained from Thai Meteorological Department (TMD) which includes daily rainfall, relative humidity, class a pan evaporation, minimum and maximum temperature measured from 3 main stations of Nakhon Ratchasima provinces from 1986 to October 2016. For 2 local stations, Bua Yai and Sida, available daily rainfall data gathered were from 1996 to 2016 and 2005 to 2014, respectively (see spatial location map of each station in Figure 2-3).

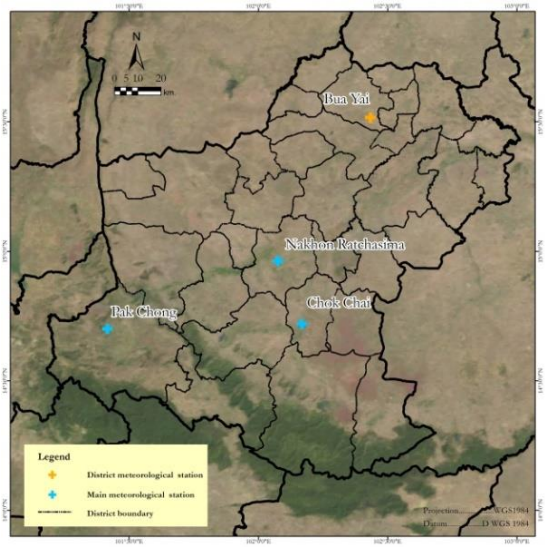

Figure 2-3: The locations of 3 main stations and a local station in Nakhon Ratchasima province.

Soil data

Soil data obtained from Land Development Department (LDD) are composed of a 2015 soil unit map and soil property data at 1:4,000 scale. Soil unit map shows 8 classified series of soil based on Soil Taxonomy by United States Department of Agriculture, 2010. LDD staff surveyed and collected soil samples 2- meters depth using hand driven auger to determine physical and chemical properties including environmental soil. Moreover, data on hydraulic conductivity (Ksat) and bulk density of 15 point locations from the lower part of the study area are available (see spatial location map in Figure 2-4.

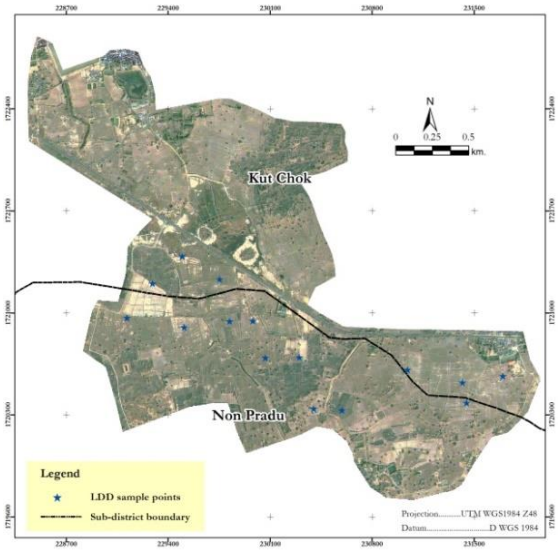

Figure 2-4: The spatial locations of LDD sample points in lower part of the study area that were recorded physical and chemical soil properties including Ksat and bulk density.

Groundwater level

Groundwater level obtained from Department of Groundwater Resources (DGR) was measured during the start of the digging activity (1987 – 2013) from 19 observed wells close to the study area in Bau Yai district. In addition, LDD staff measured groundwater level from 15 points of standpipe piezometer in 2016 located in lower part of the study area.

Vegetable data

LDD provides land use map at 1:50,000 scale made in 2012 which is based on a classified Landsat image using 11 classes of level 3 and land parcel points that recorded rice production (kilogram/rai) per parcel in 2015. These classification levels categorized particular groups of land use and land cover data and gives more detail of definitional information (Anderson et al., 1976). Department of Agriculture Extension (DOAE) provided an average main crop production such as rice cassava and sugar cane in province and district scales during 2010 to 2015. Moreover, root depth of rice obtained from Rice Department (RD) for 3 main genes that cultivated in the study area namely กข6, กข15 and jasmine rice 105.

For crop cycle stage monitoring, this research use normalized difference vegetation index (NDVI) map series of the PROBA-V satellite with 10-day NDVI composites product of 300 meter resolution from September 2015 to October 2016 that are provided by The European Space Agency (ESA). The product values are in the digital number (DN) values range from 0 to 255. Normally NDVI value range from +1.0 to -1.0 depend on land cover types in that area(USGS, 2015) A conversion from DN range to physical range needs scaling factor and offset value as defined in Table 2-3 and is retrieved by follow equation (Jacobs et al., 2016):

$$PhyVal = DN * scalingFactor + Offset$$

Table 2-3: Scaling factor and offset value for NDVI product version 1.

Variable	Scaling factor	Offset
NDVI	0.004	-0.1

Elevation data

Digital Elevation Model data at 5 meter resolution obtained from IDD was generated from 2004 to 2007 with a vertical accuracy of 2 meter or better in a slope area less than 35 percentage (LDD, 2010).

Remote sensing data

Synthetic Aperture Radar (SAR) data from Radarsat-2 sensor were obtained for soil moisture mapping. The sensor operates in C-band at wavelength 56 mm and frequency 5.4 GHz. This satellite was launched on December 14, 2007 for near-real time applications such as disaster management, natural resources and agriculture monitoring ("RADARSAT-2," 2016). The monthly RADARSAT-2 (MDA&CSA) images for the period September 2015 to October 2016 were provided by GISTDA.

2.2.2. Additional data

Soil samples (undisturbed and disturbed samples)

Due to limited information about soil properties such as soil texture, organic fraction, Ksat and bulk density, soil samples were collected: 24 samples of undisturbed and disturbed surface soil were collected with a stainless iron core at a top layer 5 centimeter in different soil types, especially in the northern part of study area. A stratified random technique was used to identify locations based on LDD soil type map (see spatial location map in Figure 2-5). All undisturbed samples were packed in a core sample case and transported to Geoscience laboratory (GSL) of Faculty of Geo-Information Science and Earth Observation (ITC), University of Twente, for further analysis.

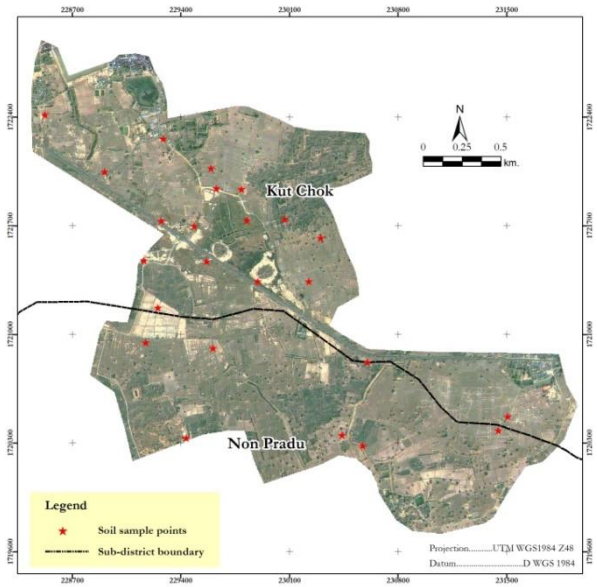

Figure 2-5: 24 collected points for soil samples in the study areas.

2.3. Methodology for research objectives

The research methodologies that were applied to achieve 3 specific objectives are described below in more detail and shown in Figure 2-6.

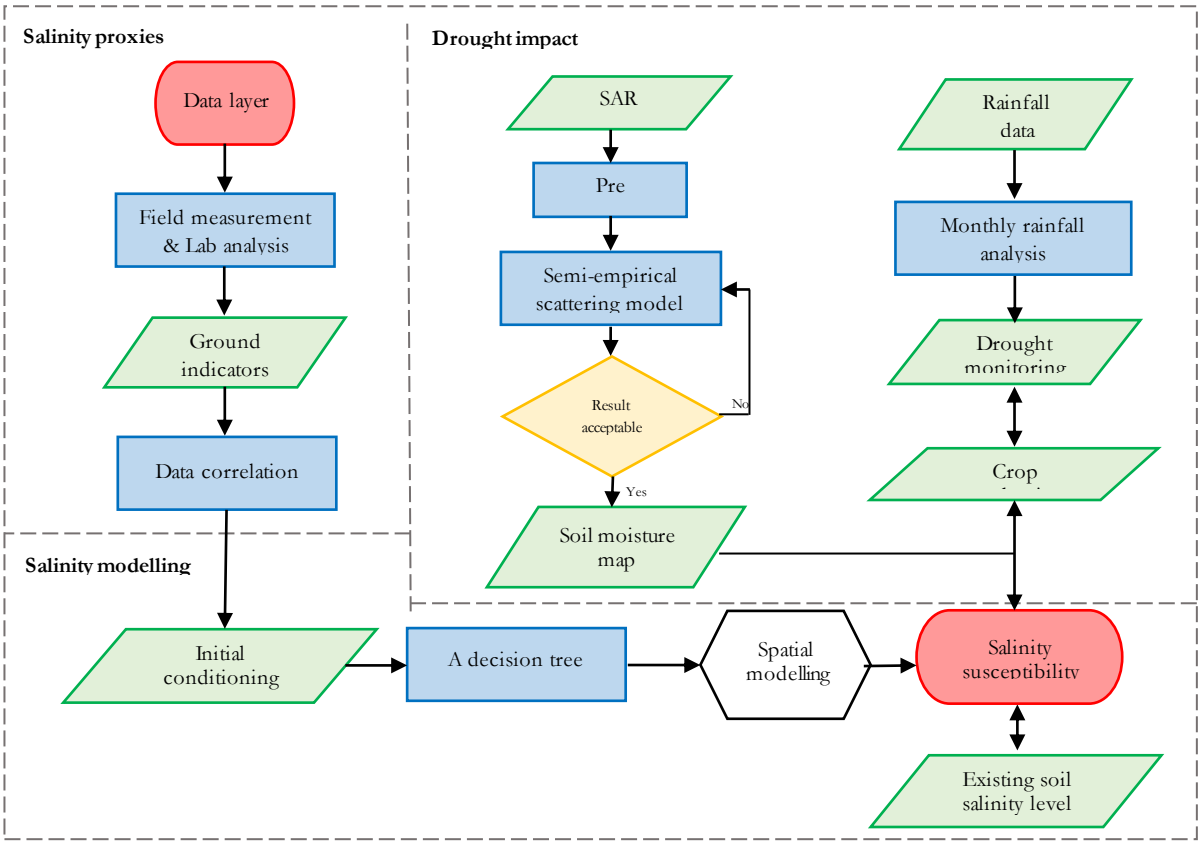

Figure 2-6: Methodological flow chart of this research.

2.3.1. Research Objective 1: To establish salinity proxies using local information of vegetation types, elevation, soil properties and soil moisture state to soil salinity

It involves 3 main steps as follow: field method, data analysis and data correlation to implement for reach this objective and answer related research questions.

2.3.1.1 Field method

The fieldwork operation was made during September 19 to October 21, 2016 to collect undisturbed soil samples, measurement of Electrical Conductivity (EC), soil moisture (SM) values and NDVI values and gathering current information about soil salinity, crop growth and crop production.

Soil moisture measurement

The soil moisture content was directly measured on soil surface by using a sensor tool called W.E.T. (Water Content Electric Conductivity Temperature). Three rods generate a 20 MHz signal and produce a small electromagnetic field within the soil to determine dielectric properties that are detected by the W.E.T. sensor (Delta-T Devices Ltd, 2007). The sensor converts the measured dielectric properties into soil moisture content over the full range, 0 to 80 % of soil pore space. The distribution of sampling points was selected by stratified random sampling using land use and soil texture maps. A total of 109 points were measured (Figure 2-7).

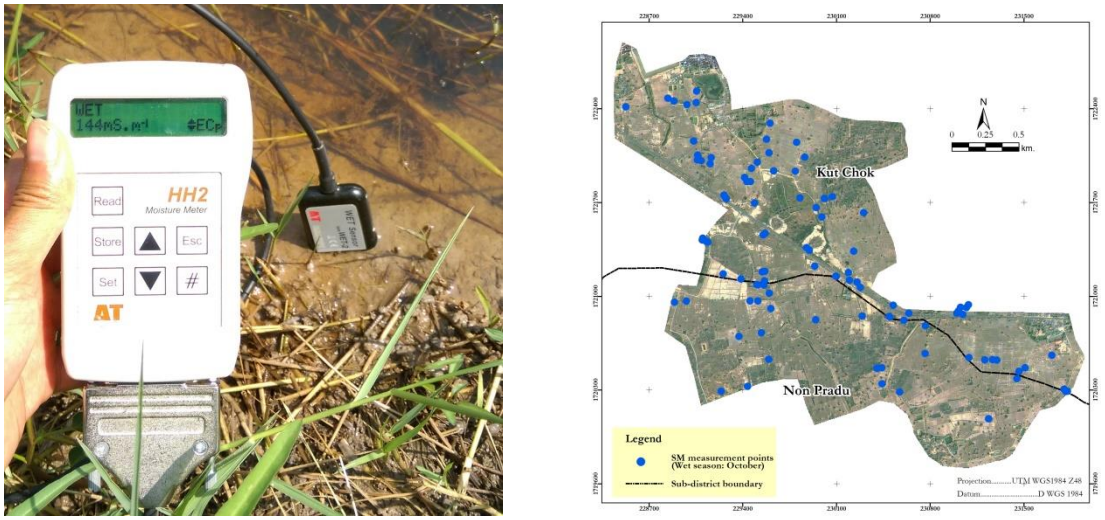

Figure 2-7: SM measuring in the fieldwork and spatial locations of SM points in wet seasons.

Electric conductivity (EC) measurement

The electric conductivity (EC) was also measured by W.E.T. tool with the same process as soil moisture content. Electrical conductivity of water (in $mS.m^{-1}$) within soil pores is determined by the concentration of different ions within the pore water and by the temperature that calculated using a unique formula to reduce effects of probe contact and soil moisture during measurement (Delta-T Devices Ltd, 2007). The same amount of SM and EC points were used as database in wet season. For dry season, EC values obtained from LDD database that recorded during 21 - 29 January 2016 (Figure 2-8). So, EC values are categorized by Food and Agriculture Organization (FAO), 1976 to represent soil salinity concentration for plant response into 5 groups as shown in Table 2-4.

Table 2-4: Salinity category according to EC value for plant response to soil salinity.

EC values ($dS\ m^{-1}$)	Soil salinity class	Effect on crops
0 - 2	Non saline	Negligible effects for plants
2 - 4	Slightly saline	Restricted growth for sensitive plants
4 - 8	Moderate saline	Restricted growth for many plants
8 - 16	Strongly saline	Satisfactory growth for tolerant plants only
> 16	Severe saline	Satisfactory growth for a few very tolerant plants only

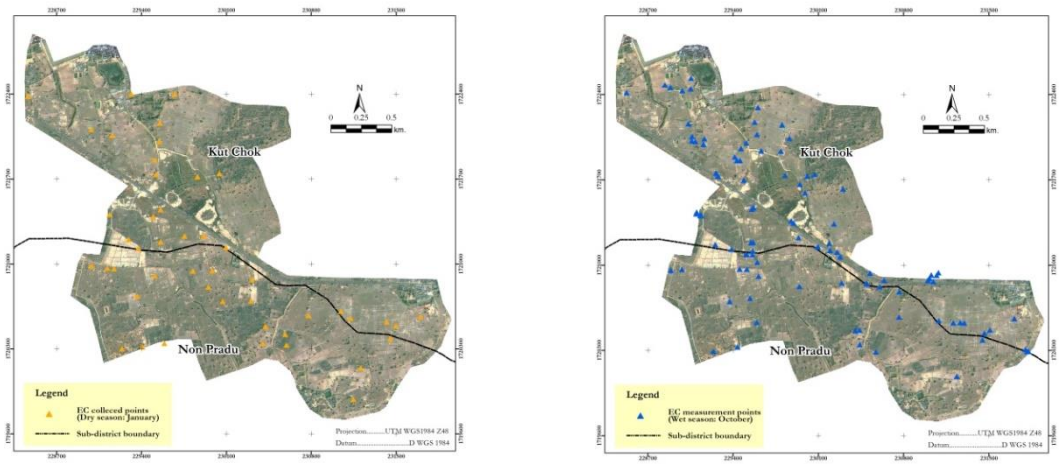

Figure 2-8: EC collected points by LDD in dry season (left) and EC measured points by sensor tool in wet seasons (right).

Field measurement of Normalized difference vegetation index (NDVI)

Normalized difference vegetation index (NDVI) was measured by Green Seeker handheld crop sensor ranging from 0.00 to 0.99. The sensor continuously scans the cover of a target area by emitting brief bursts of red and IR signals to the plant and measures the amount of energy that reflected back in each signal (Trimble, 2014). The result can simply determine vegetation health in different growth stages and crop types. 17 points were measured at least 4 times per point in various land cover during fieldwork namely cassava, corn, eucalyptus, deciduous forest, grass, paddy rice and sugarcane (Figure 2-9).

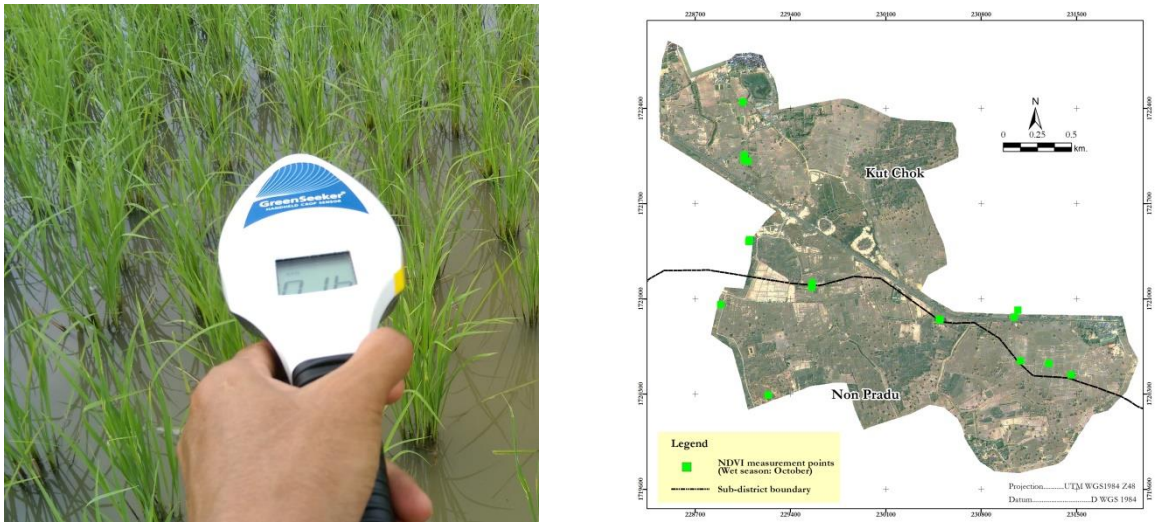

Figure 2-9: NDVI measuring in the fieldwork and spatial locations of NDVI points in wet seasons.

2.3.1.2 Lab analysis

All soil samples collected during fieldwork period have been analysed in GSL. The 24 undisturbed and disturbed soil samples were brought to the laboratory to do soil analysis for the determination of soil parameters: Ksat, BD, porosity, SM content, SOM and soil texture.

Saturated hydraulic conductivity (Ksat)

The Ksat calculation was determine using the laboratory permeameter, model M1.09.02.E of Eijkelkamp Company (Department of Transportation, 1998). First, a top side of each core sample was put in a tray filled with water until soil became saturated. The water can be sucked through top soil as a same way that happens in a field. Then, the measurement was taken within various time intervals to drain off water for each soil sample. Ksat was repeated and recorded until constant value at least 5 times that was observed in equal time interval. The following equation was used to calculate Ksat value:

$$Ksat = (V * L)/(A * h * t)$$

Where, V= volume of drain off water from soil (cm^3), L = length of soil column (cm),
h = different water level inside and outside sample core (cm), A = surface area of core sample (cm^2)
t = time interval of the measurement (min).

Bulk density (BD)

BD estimation was calculated as dry bulk density (g/cm^3). All saturated soil samples were dried continuously at 105°C at least 24 hours until the constant weight was obtained. The bulk density was calculated according to the following equation:

$$BD = Wdry/Vsoil$$

Where, Wdry = dry weight of soil core (g), Vsoil = total volume of soil core (cm^3).

Porosity

Porosity value related to amount of pore space in the soil. One of the porosity calculations uses the relationship between volume of the sample and average particle density as in this equation:

$$Pt = (1 - Pb/Pd) * 100$$

Where, Pt = porosity (%), Pb = bulk density, and Pd = average particle density of soil (2.66 g/cm^3).

Soil moisture content

The disturbed samples were weighted and then were kept inside the oven at 105°C at least 24 hours. Dry weight samples were measured after the constant weight recorded. The initial soil moisture was determined as follows:

$$SMd = (Wor - Wdry/Wdry) * 100$$

Where, SMd = dry soil moisture content (%), Wor = original weight of soil, Wdry = dry weight of soil.

Soil organic matter (SOM)

Soil organic matter of soil sample was directly determined by Loss of Ignition (LOI) method (Heiri et al., 2001) that analyzed amount of SOM by comparing the weight of a sample before and after complete burning. Thus, 4 small portions of each sample (about 0.5 g) were heated to 600 °C. in a muffle furnace. The SOM was calculated as:

$$SOM(\%) = (Wor - Wig/Wor) * 100$$

Where, Wor = original weight of soil, Wig = ignited weight of soil.

Soil texture analysis

The particle size analysis with pipette method was proposed by Van Reeuwijk, 2002 and was used to separate various size fractions of soils and determine proportion of these fractions. First, disturbed samples were aggregated by wet or dry sieving based on soil fractions. Coarse fractions (> 2 mm) were sieved off and rinsed with demineralized water and then dried it out at 40°C and weighted. After that, fine fractions (< 2 mm) of each sample were weighted out approximately 20 gram into a beaker, added 15 ml of water and H_2O_2 30% and placed on water bath (80°C) until decomposition of SOM completely. In case of removal of carbonate, hydrochloric acid and water were mixed in a beaker, so SOM was quickly decomposed with this acid. Next, these samples removed remaining H_2O_2 on hot plate, added up to 250 ml of water to the soil residue before shaking. The soil solutions were shaken for 16 hours. The fraction > 50 μm was obtained via sieving through a 50 μm sieve above a sedimentation cylinder. The sedimentation cylinder was sampled (20 ml) at different time intervals, at different depth (based on a temperature) to obtain the different texture fractions < 50 μm in 1 min, < 20 μm in 5 min, < 2 μm in 5.5 hrs. The different fractions in suspension were dried overnight at 105°C. The dry and cool fractions were weighted, while sand fractions were further sieved (1000-500-250-100-50 μm) to determine sand fraction percentages separately. In conclusion, the percentage of sand, silt and clay fractions were calculated individually as follows:

Clay (< 2 μm) = (**H** x 50) – (**Z** x 50) (wt. **K**);

Silt (2-20 μm) = (**G** x 50) – (**Z** x50) – **K** (wt. **L**)

Silt (20-50 μm) = (**F** x 50) – (**Z** x 50) – **K** – **L** (wt. **M**);

Sand (> 50 μm) = **A** + **B** + **C** + **D** + **E**

Sample weight = **K** + **L** + **M** + **N** (all weights in gram)

Where,

A (1000-500-250-100-50 μm) through **E** = weight individual sand fractions;

F= weight 20 ml pipette aliquot of fraction <50 μm

G= weight 20 ml pipette aliquot of fraction <20 μm;

H = weight 20 ml pipette aliquot of fraction < 2 μm

Z = weight 20 ml pipette aliquot of blank

2.3.1.3. Data preparation and correlation

All the data collected from different agencies came with different scale or different spatial resolutions (Table 2-2.) All the data were converted into a raster data structure with 5 meter spatial resolution which is considered as an appropriate size based on a highest resolution of datasets. Each data layer was resampled to 5 meter spatial resolution in UTM WGS84 z48N projection using ILWIS Open 3.8.5.0.

Correlation of collected data for understanding soil salinity

A basic method that approaches to understanding soil salinity progress in space and time with salinity proxies is a cross-map table and then aggregation by statistic functions based on same spatial resolution of all data layers. These data layers were imported and rasterized in ILWIS Open 3.8.5.0 and then using "Cross" operation in "Raster operation" tools. The cross operation overlaid 2 raster maps, compared values of pixels on the same positions in both inputs and gave combination values to output cross map and table. For understanding correlation for soil salinity, each cross result was plotted a box plot graph from statistics values in Microsoft Excel 2010 as seen in chapter 4.2. The statics values were calculated by using "Aggregate Column" operation within table window of an output cross table, so aggregation functions were used namely average, standard deviation, minimum and maximum.

2.3.2. Research Objective 2: To develop a spatial model predicting soil salinity based on vegetation types, elevation, soil properties and soil moisture state to soil salinity

When the correlation of all data layers had been computed and syntheses, main salinity indicators were selected and considered as main parameters for spatial modelling of soil salinity. For this purpose the concept of building decision tree was selected to fulfil specific objective2.

2.3.2.1 Initial conditioning factors

Main factors caused soil salinity enable to identify from a better correlation within sub-units or sub-types of each data layer to EC value in dry and wet season. Results of the correlations can be classed threshold values based on soil salinity categories from ranges of EC values and applied these results to make a decision tree.

2.3.2.2 Constructing a decision tree

Decision trees formalise efficiently basic approach for classification through a sequence of simple, easy-to-understand tests whose semantics are intuitively clear to domain experts (Murthy et al., 1994; Shrestha et al., 2004) Decision analysis is a simple technique based on risk , uncertainty and probabilities to model and analyse natural problems (Shrestha et al., 2004). The initial conditioning factors that introduced into a hierarchy of decision trees were soil texture, elevation, land use and NDVI. Then, soil salinity assessment was performed follow decision rules from the final trees by a raster-based GIS environment.

2.3.2.3 Spatial modelling

A simply spatial model was applicable to predict soil salinity with 4 basic data layers that were available to collect from Thai agencies or online data sources. The model was applied map overlay procedures with multiple maps in GIS environment. ILWIS Open 3.8.5.0 software also provided two-dimensional table for map calculation to combine or classify raster map. The proceeding of two-dimensional table developed from decision trees step by step use to create a soil salinity susceptibility map.

2.3.3. Obj3: To determine the impact of drought on soil salinity and crop growth using remotely sensed data by means of several drought indices and salinity proxies

2.3.3.1 Monthly rainfall analysis

This methodology was applied on the rainfall measurements at Bua Yai meteorological station which covered the period 1986 – 2016. A basic statistical analysis using Microsoft Excel 2010 is performed based on daily rainfall data. Monthly rainfall statistics were calculated for minimum, first quartile, median, third quartile and maximum values by using "quartile" function for making a box plot to identify amount of monthly rainfall in 2016 as compared with other years.

2.3.3.2 Soil moisture retrieval from active microwave remote sensing

Monthly Radarsat-2 that obtained from GISTDA were applied for SM retrieval by using semi-empirical model based on backscatter coefficient, dielectric constant and surface roughness values. Estimated results were validated with SM measurements and then analysed sensitivity of model parameters (surface roughness). Finally, temporal SM maps were produced from monthly parameters using the same model. All of the processing is described in data processing chapter at chapter 3.2.

2.3.3.3 Standardized Precipitation Index (SPI)

Drought indices as indicators are normally used to describe characteristics of drought, such as duration, severity, and spatial extent by computing numerical statistics for representing drought's severity or magnitude (Steinemann, 2003). Many variables are used for computing drought indices such as precipitation, temperature, stream flow and soil moisture to give more information for drought monitoring in national and local scales(Hayes et al., 2012). In the present study the SPI drought index is applied which is one of the most widely used indexes by fitting historical precipitation data to a Gamma probability distribution function (Mckee et al., 1993). Detail description of the application of SPI for drought hazard assessment is given in chapter 3.3, Data processing.

3. DATA PROCESSING

3.1. Soil salinity modelling

Soil salinity modeling process involved as an initial step, data correlation of salinity proxies to soil salinity using electric conductivity (EC) values to determine and clarify main conditional factors. Decision trees were then constructed based on these main factors. Using spatial modeling and the developed decision rules, salinity susceptibility was mapped in GIS environments with map overlay functions. Detailed explanation of the various steps leading to soil salinity modelling is as follows:

3.1.1. Data correlation process

The 2 main datasets were field measurement and lab analysis data and ancillary data layers such as soil EC, soil moisture, soil texture and land use which contained by point and polygon features respectively. All features are obtained attribute table that consisted of fields/columns in value or class (string) domains using for raster conversion. Rasterize operation within operations menu applied for conversion point or polygon features to grid raster with "point to raster" or "polygon to raster" functions. When all data layers had been converted to raster files, "cross" functions in rasterize operations operation were used for correlation all data layers. The basic correlation is crossing between 2 data layers; moreover results of the crossing can re-operated with other layers to give more details these correlations.

Over 30 correlation results were computed and shown in cross tables, and then these results were represented and interpreted by descriptive statistics with box plots. The descriptive statistics were calculated from "aggregate column" operation in table window of cross tables, so this operation got many dialog box options to settings. Column option uses to aggregate values of the whole column to obtain one output value, function option is the important option for selecting statistic functions to aggregate values in a column per group and group option is chose for grouping the values of a column rely on a class domain. Main 4 statistic functions that calculated in a now column were average, minimum, maximum and standard deviation values.

The descriptive statistics were duplicated and plotted on a box plot by using Microsoft Excel 2010. Only main correlations that related and affected to soil salinity were illustrated data correlation results in chapter 4.2 and implemented for the decision trees.

3.1.2. Decision trees constructing

The results obtained in the analysis of indicators for soil salinity show 4 main factors namely soil texture, relative elevation variation in the area, land use and vegetation cover (NDVI). From this result it was possible to make a spatial model for assessing soil salinity hazard. For this purpose a decision tree model was considered very efficient. For hazard assessment, the decision trees can be utilized for hazard classifications by ranking and considering importance causal and conditioning factors for spatial modelling (Shrestha et al., 2004). A decision tree consists of internal node that splits the class into subsets of classes by using appropriate criteria with the corresponding threshold values for the classification, so the decision tree classifiers are successful approaches to decision making process (Safavian & Landgrebe, 1991). The decision trees set hierarchy level of evidence that sequenced impact factors to soil salinity progress of the study area as seen in Figure 4-9.

3.1.3. Spatial modelling

In order to implement the decision tree all the map layers were resampled to 5 meter spatial resolution without loss of significant information based on a high resolution of datasets. ILWIS Open 3.8.5.0 software is used to implement the decision tree to create soil salinity map. In ILWIS, "two-dimension

tables" operation is used to combine or reclassify 2 raster maps from a specific class or domain. The two-dimension tables were created by using primary and secondary domain of 2 raster inputs and gave initial value from new domain. This function was first operated for 2 raster maps and then used the result as input map to reprocessing with another raster map. The salinity susceptibility result was classified into 5 classes; very high, high, moderate low and none. Following expression was used in the command line of the main window in ILWIS:

$$OutMap = Two - DimTableName[Inmap1, Inmap2]$$

Where, OutMap is name of output map, Two-DimTableName is name of two-dimension table, Inmap1 is name of input raster map1 and Inmap2 is name of input raster map2

3.2. Soil moisture retrieval from active microwave remote sensing

The variability of soil moisture (SM) could be a measure for salinity by using characterization of active microwave imagery and backscattering constants (Metternicht & Zinck, 2003). First step involves the calculation of backscattering coefficient for convert pixel values to a physical quantity in decibel (dB) unit (Dubois et al, 1995). Second, constant values are identified from a simple linear regression illustrating the relationship between the backscattered signal and dielectric property of soil and surface roughness of different vegetation types. SM retrieval form SAR image was applied the semi-empirical scattering models which proposed by Das & Paul, 2015. Compared to other models, semi-empirical scattering models consider several variables such as measured soil moisture, vegetation and soil texture to obtain soil moisture values with a higher accuracy, low root-mean-square error (RMSE) and high confidence level (Das & Paul, 2015). Validation is done by comparing SM estimated values and SM from ground measurements. Finally, the model is applied for SM retrieval with other temporal SAR images in order to identify levels of SM from January to October, 2016. SAR data processing is described in detail as follows:

3.2.1. Geometric and Radiometric correction

Initially Radarsat-2 images acquired in 2015 and 2016 were in the format of Standard Georeferenced Fine (SGF). So data is already georeferenced with standard coordinate system at top left corner of the image, geometric correction was used for geocoding images with elevation data from Shuttle Radar Topography Mission (SRTM) DEM. After this radiometric calibration was applied with physical parameters from header files (*NEST 5.1 User Manual*, 2014).

3.2.2. Backscatter coefficient (σ°)

Radar system measures the amount of radiation transmitted and scattered back through microwave signal from the earth surface to antenna and then receiving signal is recorded. A pixel of radar image contains a digital number (DN) corresponding to the amplitude of the backscatter radiation (*ITC Corebook*, 2013). The backscatter coefficient represents the radiation losses from surface materials that produce different scattering levels and therefore considered as an important factor for soil moisture extraction from SAR image. These backscattering coefficients ($\sigma°$) were calculated by using calibration constant (K_{db}), incidence angle in pixel position (i_p) and at scene center (i_{center}) following equation (Das & Paul, 2015):

$$\sigma°(db) = 20log_{10}(DN_p) - K_{db} + 10log_{10}\left(\frac{\sin(i_p)}{\sin(i_{center})}\right)$$

3.2.3. Dielectric constant (ε)

Normally microwave energy relates to mechanisms between the electric field and dielectric materials that are expressed to an electric permittivity of free space as either a dielectric constant or relative permittivity (Mcnairn et al., 2010). The dielectric constant depends on the moisture content in soil and vegetation

which can be calculated by polynomial expressions using volumetric moisture content (Mv), percentage of sand (s) and clay (c) for each sample by weight (Hallikainen et al., 1985).

$$\varepsilon = (a_0 + a_1 s + a_2 c) + (b_0 + b_1 s + b_2 c) Mv + (c_0 + c_1 s + c_2 c) Mv^2$$

The frequency dependent coefficients (a_i, b_i, and ci) of imagery part in c band wavelength shown in Table 3-1. So the dielectric constant was calculated based on the volumetric moisture content values from lab analysis and field measurement, the MV values of 14 soil samples and 52 measurement points ranged from 0.27 to 0.89 m^3/m^3

Table 3-1: the frequency dependent coefficients of 6 GHz in imagery part.

Frequency, GHz	a_0	a_1	a_2	b_0	b_1	b_2	c_0	c_1	c_2
6	-0.123	0.002	0.003	7.502	- 0.058	- 0.116	2.942	0.452	0.543

3.2.4. Surface roughness (r.m.s.)

Surface roughness is represented by surface height variations compared to a smooth reference surface (Srinivasa Rao et al., 2013). Effect of surface roughness is an important parameter for soil moisture extraction from SAR images (Ulaby et al., 1978). Normally, surface roughness is directly measured in a field by using standard methods with specific tools such as a chain method with roller chain, so each training plot need at least 2 or 4 distance measurements in perpendicular direct to extract roughness data (Saleh, 1993; Thomsen et al. , 2015). Moreover, surface roughness can be estimated from a multi-polarization approach using cross polarization ratio (Srivastava et al., 2008; Oh et al., 1992). In this research, surface roughness is retrieved by cross polarization ratio between HV/HH.

3.2.5. Semi-empirical model

For the current research the semi-empirical scattering models was selected as a specific approach for extracting SM from Synthetic aperture radar (SAR) images with the backscattering coefficients in different vegetation and soil parameters. A multiple linear regression was formulated from backscatter coefficients, dielectric constant and surface roughness as independent variables with specific constants to extract soil moisture level by using the equation described by Das & Paul, 2015 as follows:

$$Mv\left(m^3/_{m^3}\right) = -5.63 \times 10^{-2} - 1.91 \times 10^{-4} \times \sigma^{\circ}(HV) + 8.84 \times 10^{-4} \times \sigma^{\circ}(HH) + 3.27 \times 10^{-2} \times \varepsilon + 7.47\delta \times 10^{-4} \times RMS$$

Where, Mv is estimated soil moisture,

$\sigma^{\circ}(HV)$ and $\sigma^{\circ}(HH)$ are backscattering coefficients of dual polarizations,

ε is dielectric constant and RMS is surface roughness.

Model validation

Model validation had been processed to determine degrees of confidence level for the accuracy and limitation of model simulation results compare with an accurate depiction of the real world (Aaen et al., 2007). A linear regression approach usually apply for the model validation in the environmental science literature using scatter plots of experimental observation against model prediction (Hills & Trucano, 1999). Estimated SM results from the semi-empirical model were validated with SM field measurement values. For this purpose, the cross map table from ILWIS Open 3.8.5.0 software was used.

Sensitivity analysis

Sensitivity analysis is one of the methods to characterize uncertainty in model parameters by changing one parameter keeping other constants and evaluate the sensitivities of the model predictions (Hills & Trucano, 1999). For the semi-empirical model, surface roughness parameter was selected to test sensitiveness to the model because this parameter was extracted from cross polarization ratio without ground height measurements. The calculated values were plotted to show increasing percentages of SM with different values of surface roughness which are increased by 20 %. The "Raster Calculate" function in "Spatial Analyst" tools of ArcGIS 10.4.1 was used to calculate changing values of the surface roughness parameter.

3.2.6. Soil moisture maps map on monthly basis

The SM equation was formulated from 3 model parameters responding SM percentage within acquisition time condition, so monthly SM mapping required theses model parameters which are measured and estimated during the period of time. The backscatter coefficient and surface roughness parameters enabled to estimate from SAR images while dielectric constant calculation is based on sand and clay percentages and soil moisture content in time of data acquisition.

3.3. Long term climatic data processing

The emphasis of the present research is mainly agricultural drought and drought impacts on soil salinity. In this research, monthly rainfall data analysis and the Standardized Precipitation Index (SPI) were selected for drought hazard assessment. The monthly rainfall analysis was computed and illustrated monthly rainfall distribution to define dry and wet periods of the study area and to compare with amount of accumulation rainfall in 2016. SPI is the most suitable for this research that based only on rainfall data while some indices required more inputs such as soil moisture or evapotranspiration (Guttman, 1998), so Bui Yai station also recorded only rainfall data. Moreover the SPI results normally use to categorize drought situations with standard intervals to reflect water resource situations soil moisture and ground water for agricultural drought impact to soil salinity.

3.3.1. Monthly rainfall analysis processing

Daily rainfall data was measured at Bua Yai station (latitude 15.60 north; longitude 102.45 east). The daily rainfall data was collected in digital format from January, 1986 to October, 2016 with separate excel worksheets that summarized and computed statistical values to create total monthly rainfall boxplot in Microsoft Excel 2010. Summary monthly rainfall data in all years was rearranged in a new worksheet and then selected "minimum", "first quartile", "median", "third quartile "and "maximum "functions under formulas tool bar to calculate these statics values in every years. The box plots displayed different ranges of accumulated rainfall over 25 percentile of median value and under 25 percentile of median value, and then monthly rainfall values in 2016 were pointed on the monthly rainfall boxplot to compare amount rainfall in 2016 with other years.

3.3.2. Standardized Precipitation Index (SPI) calculation

In this research, drought index was calculated using SPI by Mckee et al., (1993). SPI can be calculated as a short-term SPI that defines meteorological and moisture conditions for agriculture in short timescales of precipitation from a week to 6 months and a long-term SPI that associates with anomalous stream flows, reservoir and groundwater levels and hydrological drought applications (World Meteorological Organization, 2012). The 3-month and 6-month SPI were selected to relate with soil moisture and groundwater levels in 2016 respectively.

In calculating SPI, the following variables needed include the mean of the precipitation from Bua Yai station covering the 30-year period as well as statistics U, shape and scale parameters of Gamma distribution. The mean precipitation for the time frame was based on the result of the moving window method for 3-months and 6-months period. The mean can be computed using the equation below.

$$Mean = \bar{x} = \frac{\sum x}{n}$$

Where, x is precipitation,

n is the number of precipitation observations.

The precipitation value is then converted to lognormal values and the statistics U, shape and scale parameters in order to compute the gamma distribution.

$$\alpha = \frac{1}{4A}\left(1 + \sqrt{1 + \frac{4A}{3}}\right)$$

$$\beta = \frac{\bar{x}}{\alpha}$$

and

$$U = \ln(\bar{x}) - \frac{\sum \ln(x)}{n}$$

Where, $\alpha > 0$, $\beta > 0$ and $x > 0$

α is shape parameter,

β is scale parameter.

Then using parameter results, cumulative probability of the event is calculated for each station by using the given formula:

$$G(x) = \int_0^x g(x)dx = \frac{1}{\beta^{\alpha}\Gamma(\alpha)}\int_0^x x^{a-1}\, e^{-x/\beta}\, dx \qquad \Gamma(\alpha) \text{ As the gamma distribution function}$$

In general, typical precipitation will have Gamma distribution or distribution function. Since the gamma function is undefined for $x = 0$, a precipitation distribution may contain zeros or no precipitation report. So the cumulative probability becomes a following function.

$$H(x) = q + (1 - q)G(x)$$

Where, the probability is zero and approximately $q = m/n$ (m: number of days with no precipitation and n: total number of days).

The cumulative probability is then transformed to standard normal random variable z with mean zero and variance of one. However, SPI primarily considers total precipitation, cumulative probability density function of total precipitation must be considered then transform to standard normal Z (Abramowitz & Stegun, 1964).

$$Z = SPI = -\left(t - \frac{c_0 + c_1 t + c_2 t^2}{1 + d_1 t + d_2 t^2 + d_3 t^3}\right) \quad \text{for } 0 < H(x) \leq 0.5$$

$$Z = SPI = +\left(t - \frac{c_0 + c_1 t + c_2 t^2}{1 + d_1 t + d_2 t^2 + d_3 t^3}\right) \quad \text{for } 0.5 < H(x) \leq 1.0$$

Where,

$$t = \sqrt{\ln \frac{1}{(H(x))^2}} \quad \text{for } 0 < H(x) \leq 0.5$$

$$t = \sqrt{\ln \frac{1}{(H(x))^2}} \quad \text{for } 0.5 < H(x) \leq 1.0$$

$$c_0 = 2.515517$$

$$c_1 = 0.802853$$

$$c_2 = 0.010328$$

$$d_1 = 1.432788$$

$$d_2 = 0.189269$$

$$d_3 = 0.001308$$

Required SPI will be obtained and use to classify severity level as specified (Naresh Kumar et al., 2015). The SPI result values were classified into 7 categories as shown in Table 3-2 (Mckee et al., 1993).

Table 3-2: Drought category according to SPI value.

SPI values	Category
2.00 +	Extremely wet
1.50 to 1.99	Very wet
1.00 to 1.49	Moderately wet
-0.99 to 0.99	Near normal
-1.00 to -1.49	Moderately dry
-1.50 to -1.99	Severely dry
-2.00 and less	Extremely dry

4. RESULTS AND DISCUSSION

4.1. Analysis of ground indicators

The indicators for soil salinity were measured in the field and analysed in the laboratory. The indicators considered important are electrical conductivity of soil, soil moisture content, NDVI, land cover/land use and relative elevation in the terrain. These indicators were calculated and simulated by specific approaches or processing and then implemented for soil salinity progress and assessment.

From the field measurement, EC values range from 0.17 to 23.07 while SM values ranged from 15.50 to 79.80% . These values are categorized into 5 classes as defined in Table 2-4 and the descriptive statistics of each salinity class are summarized in Table 4-1. The EC values are positively related to types of soil texture, so 40% of measurement points distributed all over the study area were grouped in a non-salinity class and only 5% was classed into a severe salinity level sited on fine textured soil areas. EC result versus SM results show a negative correlation which means % SM slightly decreased when EC amounts gradually increased (Figure 4-1). Moreover, comparison of the EC values between dry and wet season in Table 4-1 indicate a more than two-fold decrease of the maximum EC value from dry to wet season, the highest EC points occurred at almost the same location of fine soil at middle of the study area.

NDVI values range from 0.09 to 0.80. The lowest NDVI value was collected within a paddy field area in tillering stage with 40 cm height covering 80 % of water area and 20% of the rice sprouts. The highest NDVI value was recorded over a 3 month cassava plantation with 1.50 m height covering 95% of cassava tree and 5% of soil. The NDVI value range in the study area is assigned to salinity classes specifically none saline and slightly saline (Table 4-1). As higher NDVI values have lower EC values, it is categorized into non-saline class.

Table 4-1: Values of soil salinity indicators as measured from the field in 2016.

Salinity classes		Field measurements			
		EC (dS/m) (Dry season)	EC (dS/m) (Wet season)	SM (%)	NDVI
Non saline	Min	0.13	0.17	15.77	0.42
	Max	1.94	1.97	75.40	0.80
	Mean	**1.04**	**1.06**	**49.75**	**0.59**
	SD	0.60	0.51	13.60	0.10
Slightly saline	Min	2.25	2.03	21.87	0.09
	Max	3.94	3.93	78.09	0.44
	Mean	**3.13**	**2.86**	**48.18**	**0.27**
	SD	0.71	0.61	8.30	0.18
Moderate saline	Min	4.06	4.06	22.49	-
	Max	6.22	7.88	63.05	-
	Mean	**5.00**	**6.09**	**46.97**	-
	SD	0.88	1.29	4.50	-
Strongly saline	Min	9.19	8.20	29.40	-
	Max	13.76	15.81	52.59	-
	Mean	**11.32**	**11.17**	**44.69**	-
	SD	1.82	2.58	4.10	-

Severe saline	Min	42.06	17.51	29.60	-
	Max	52.44	23.07	40.80	-
	Mean	**47.25**	**20.35**	**35.42**	-
	SD	7.34	2.58	2.70	-

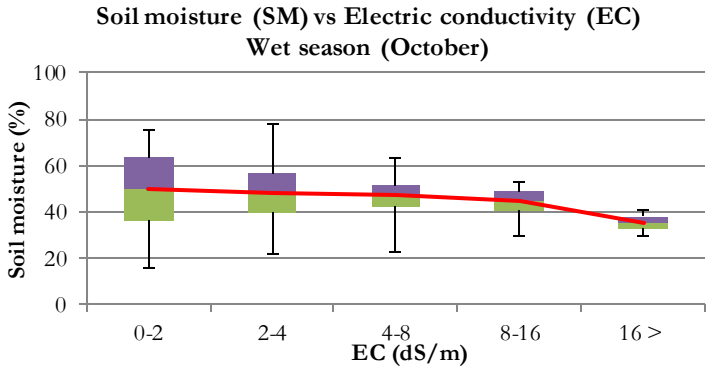

Figure 4-1: Correlation between soil moisture and electric conductivity values as presented in Table 4-1.

EC measurement values presented as soil salinity levels closely relate with soil minerals, climate and soil properties which directly affect crop yields, crop suitability and plant nutrient availability (Bobby et al., 2009; NRCS, 2014). To identify the soil texture units, soil physical properties such as saturated hydraulic conductivity (Ksat), bulk density (BD), porosity and organic matter (SOM) were analyzed in ITC laboratory (FAO, 2016). These properties were then related with EC measurement values as seen in Table 4-2.

Ksat, one of the most important soil properties refers to ability to transmit water through pores between particles by increasing soil water content until reaching a maximum rate with saturated conditions (Thomas & Galbraith, 2016). The Ksat values can indicate permeability rates to describe the downward movement of water through soil horizons, so a higher conductivity rate means a higher permeability. Determined Ksat values gave a lower average value (14mm/hr.) in fine textured soils and higher average value (35mm/hr.) in coarse textured soils, therefore water can be more permeable through coarse textured soils than fine textured soils. Ksat values ranged from 0 to 72 mm/hr while SOM values range from 0.39 to 41.7.

Soil BD and porosity reflect size, shape and arrangement of particles and pore spaces (Soil Quality, 2017) and optimum movement of air and water through the soil with rate and percentage of specific values (Hunt & Gilkes, 1992). Sandy soil usually has a higher BD than fine, silt or clay soils (Soil Quality, 2017). Lab results also showed a lower BD (1.23 – 1.33 g/cm^3) in fine soils and a higher BD in coarse loamy soils (1.52 – 1.77 g/cm^3). Typically, porosity ranges between 30 and 70% for soil depending on packing density (Nimmo, 2013), porosity lab results fit within these ranges with values from 33.19 to 53.56%. With lower porosity (33 -42%) found in coarse loamy soils and higher porosity (49 – 53%) got in fine soils.

SM contents were analysed in the lab resulting in a range from 1.43 to 32.45% where coarse textured soils had a lower SM percentage than fine textured soils with some overlap, results range of 1.43 to 19.28% and 15.34 to 32.44% respectively. SM is affected by texture since fine textured soils have smaller particles, hence higher surface area, and enlarged capability of retaining moisture (Department of Environment & Management, 2011). As illustrated in Table 4-2, the amount of soil moisture can be correlated to salinity as well. It shows that as SM increases, soil salinity also increases.

SOM shows a relationship between clay and silt content in many sites of the tropics that directly affected by precipitation and temperature (Feller et al., 1997; AZLAN et al., 2012). The lab results revealed that fine silty soil has the highest percentage of SOM at 4.17 %. This is attributed to restricted aeration in finer-

textured soils, reducing the rate of organic matter oxidation, and the binding of humus to clay particles, further protecting it from decomposition. Additionally, plant growth is usually greater in fine-textured soils, resulting in a larger return of residues to the soil (Mccauley, 2009). Furthermore, the percentage of SOM and clay is related to the capacity of soil to the exchange of positive charged ions as cation exchange capacity (CEC)(NRCS, 2014), CEC values have a positive correlation with soil EC values (Lund et al., 1999).

Table 4-2: Correlation of measured soil physical properties with salinity.

Salinity classes		Soil properties					
		Ksat (mm/hr)	BD (g/cm^3)	Porosity (% vol)	SM (% wt)	SOM (% wt)	Clay %
Non saline	Min	6.65	1.47	33.20	1.43	0.46	0.78
	Max	52.71	1.78	44.94	19.29	2.83	4.87
	Mean	**29.96**	**1.62**	**39.23**	**9.97**	**1.32**	**2.65**
	SD	17.30	0.10	5.00	9.70	1.30	1.79
Slightly saline	Min	0.00	1.24	36.52	15.35	1.34	0.10
	Max	72.79	1.69	53.56	26.69	6.45	16.04
	Mean	**25.27**	**1.47**	**44.76**	**21.93**	**4.04**	**9.54**
	SD	24.80	0.20	6.30	5.90	2.50	8.36
Moderate saline	Min	3.58	1.34	34.20	15.26	2.19	5.03
	Max	45.86	1.75	49.66	32.45	3.81	6.45
	Mean	**22.65**	**1.57**	**40.81**	**23.55**	**3.00**	**5.83**
	SD	21.90	0.20	6.80	8.60	1.10	0.73

Soil texture analysis is done to quantitatively determine particle sizes to classify soil textural classes (FAO, 2006) which is used to benchmark how EC data relates soil salinity levels (Bobby et al., 2009). Laboratory results such as percentages of soil particles vary from Land Development Department (LDD) and may be attributed to different sampling and analytical methodologies. GSL uses pipette method to determine soil texture while LDD utilizes hydrometer method.

Based on laboratory result it is shown that clay soil normally has higher EC values because salt can be leached from the root zone and accumulates on the surface by rising of ground water with capillary force (Seeboonruang, 2013b).

4.2. Data correlation results

As the materials and method in previous chapter and achievement of the main objective needs to correlate all of the main factor maps for establish salinity proxies using local information and implement these results for developing a spatial model to predict soil salinity.

4.2.1. Correlation analysis

Statistical results are plotted to present the correlation between each factor to the EC measurements with positive and negative relationships between the dry season (21-29 January 2016) and wet season (3-12 October 2016), as shown in Figure 4-2 to Figure 4-8.

Soil texture

As seen in the box plot figures showing EC values against soil texture classes, loamy soil has gradual a change of mean EC value in both seasons while the mean EC values of fine and silty soils sharply decrease when comparing in dry and wet season. The fine soil has the most impact on soil salinity than other soils. According to Fetter, (1994), fine texture has the highest capillary rise in sediments that makes saline water

more likely to move to the soil's surface easily. Fine textured soil has high salinity because generally, salts tend to attach to clay particles, so clay soils tended to be more saline for longer (Rycroft et al., 1995).

Soil salinity level in January is higher than October because during dry season shallow saline groundwater can still move upward near the soil surface through the capillary fringe. Moreover, soils are still deeply cracked after the harvest period during this time and these cracks serve as conduit for saline water to leached upward (Kotb et al., 2000).

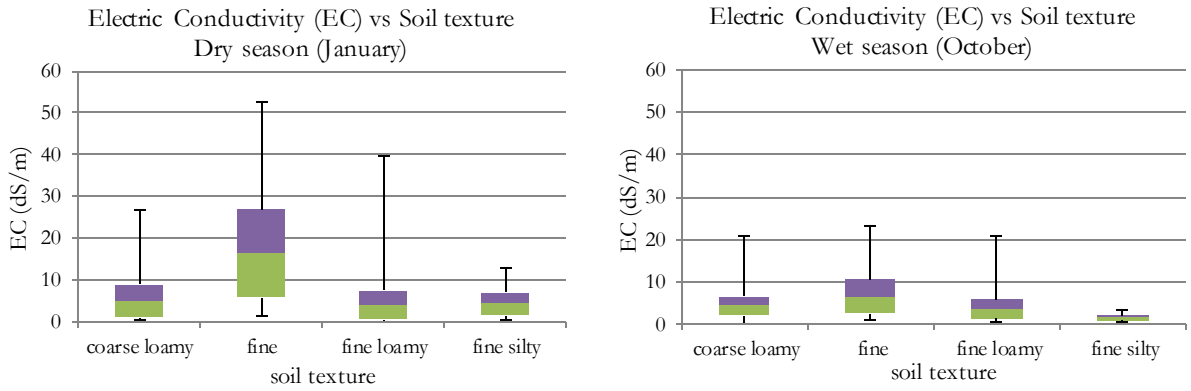

Figure 4-2: Contrast factor for soil texture classes from LDD and soil salinity with EC values in wet season and soil texture from LDD.

Organic matter

EC value correlates with many soil properties including organic matter level(Bobby et al., 2009). USDA, 2011 revealed that where organic matter and nutrients accumulated in agricultural fields, these areas have higher ECs than surrounding areas. In Figure 4-3, high amounts of organic matter also show high EC values, so high organic matter are found in fine and fine silty soils. Typically, high organic matter results to poor drainage which leads to waterlogging thus increasing soil salinity (USDA, 2011). Additionally, under saline soils, the available fraction of potassium (K) increases as cation exchange capacity (CEC) increase which is linked to organic matter content (Diacono et al., 2015).

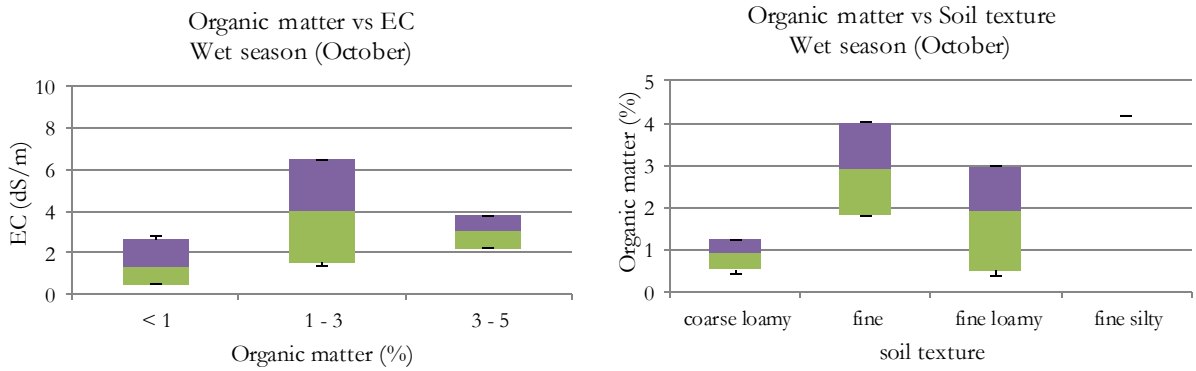

Figure 4-3: Contrast factor for organic matter classes from lab analysis and soil salinity with EC values in wet season and soil texture from LDD.

Ksat

Ksat classes refer to permeability of soil with hydraulic gradient as the driving force causing groundwater to move in soil (Department of Environment & Management, 2011). Salinity occurs because groundwater

flow is restricted and limits leaching so that salt accumulate over the periods. It means that soil with low Ksat has a higher chances of having high salinity.

The mean values of Ksat classes sharply decrease when the EC values continuously decrease in dry season, while EC values are almost at the same levels in all Ksat classes during wet season shown in Figure 4-4. So, the lowest class of Ksat values has a higher range of EC in both seasons. Ksat values directly impacts on soil salinity with an inverse relationship based on soil texture. Soil with high clay content generally has a lower Ksat than sandy soil because the pore size distribution in sandy soil favors large pores even though sandy soil usually has higher bulk density and lower total porosity than clayey soil (USDA, 1951) corresponding with correlation results between Ksat and soil textures from LDD.

Table 4-3: Saturated hydraulic conductivity (Ksat) classes (USDA, 1951).

Class	Saturated hydraulic conductivity (Ksat)	
	(µm/sec)	(mm/hr)
Very High	> 100	> 360
High	10 - 100	36 - 360
Moderately High	1 - 10	3.6 - 36
Moderately Low	0.1 -1	0.36 -3.6
Low	0.01 - 0.1	0.036 – 0.36
Very Low	< 0.01	< 0.036

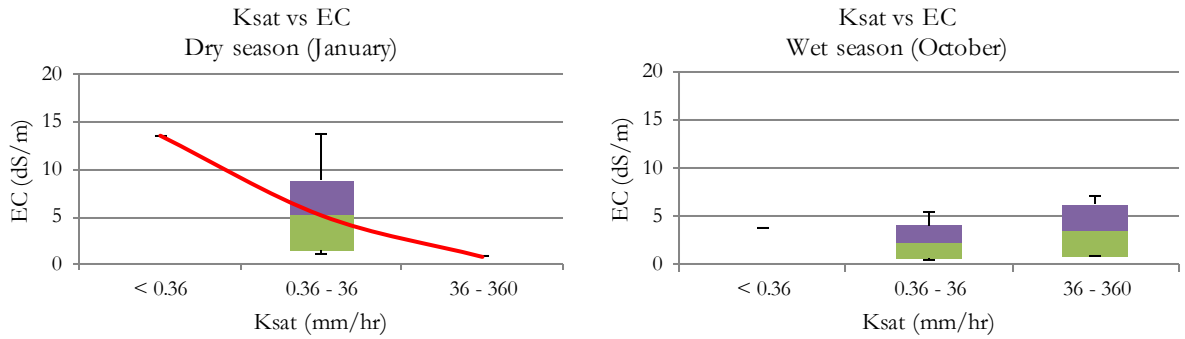

Figure 4-4: Contrast factor for Ksat classes from lab analysis and soil salinity with EC values during dry and wet season.

Land use

To relate between land use with EC values, 4 types of land use that have been effected from soil salinity by abrupt decreasing of mean EC values from wet season to dry season are cassava, eucalyptus, "rice paddy/marsh and swamp" and "marsh and swamp" respectively as can be seen in Figure 4-5. Cassava and eucalyptus, cultivated in higher elevation areas (Figure 4-6), have soil generally low in EC values because of the effect of salt being washed by rain and transported by runoff water to lowlands.

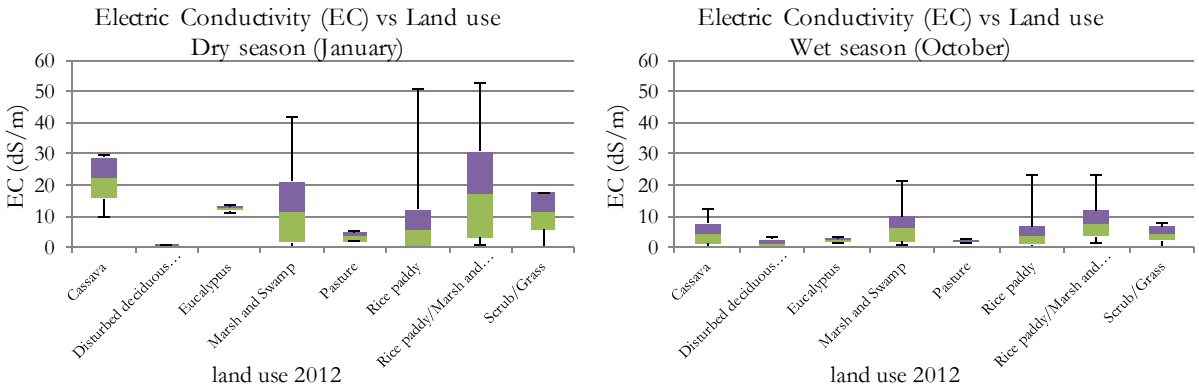

Figure 4-5: Contrast factor for 2012 land use from IDD and soil salinity with EC values during dry and wet season.

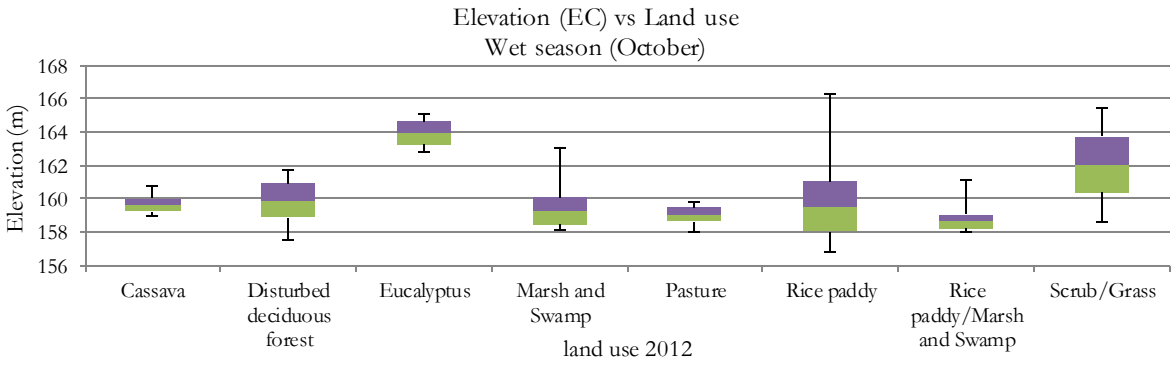

Figure 4-6: Contrast factor for 2012 land use and elevation data from IDD during dry and wet season.

DEM and soil texture

During field work and with knowledge from LDD staff and local people, soil salinity usually occurs in lower parts in the terrain. To establish the relation between soil texture, salinity and terrain, a cross-map was made between DEM, EC values and soil texture. The DEM was categorized into 5 classes with 2 meter interval based on height accuracy. The result shows a significant change of EC values in lower elevation (157-161 meters) during 2 seasons especially in a fine soil (Figure 4-7).

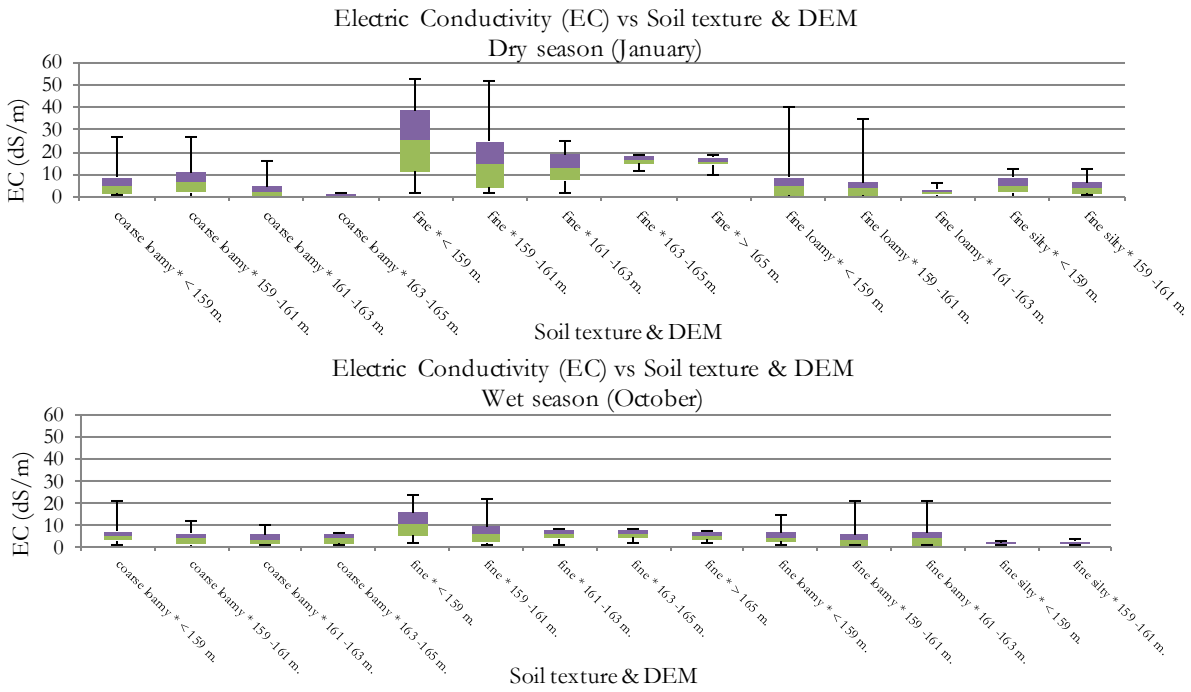

Figure 4-7: Contrast factor for soil texture with DEM for soil salinity with EC values during dry and wet season.

NDVI

In wet season, NDVI values show an inverse trend with EC classes. When salinity levels increase, NDVI values slightly decrease as seen in Figure 4-8. Soil salinity significantly affects plant growth and is indicated by darker leaves instead of their normal color, smaller leaves and stems, yellow leaves until death of leaf edges(Pitman & Läuchli, 2002). NDVI as an indicator is useful to monitor vegetation health in relation with soil salinity, with lower NDVI values corresponding to high salinity levels (Peñuelas et al.,1997). For dry season, NDVI values show almost no difference in range of salinity levels since the crops are already harvested.

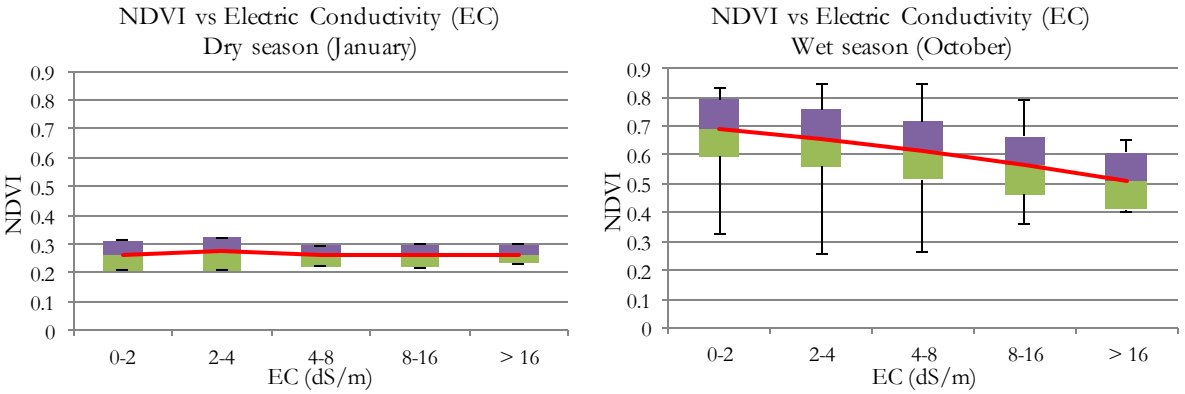

Figure 4-8: Contrast factor for NDVI values from the PROBA-V satellite data for soil salinity with EC values during dry and wet season.

4.3. Results of spatial model for soil salinity

The spatial model has been developed by incorporating the results obtained in correlation of soil salinity indicators e.g. soil texture, elevation, land use and NDVI to EC values.

4.3.1. Initial conditioning factors

The conceptual model of soil salinity designed for integrating current or available data sources to implement and monitor soil salinity in local scale is based on the criteria as shown in Table 4-4.

Soil texture is an important parameter for assessing soil salinity in rock salt beds zone such as the study area. The 4 types of soil texture are fine, fine loamy, fine silty and coarse loamy. Severe and strongly salinity occurred in fine textured soil especially in wet season, so fine texture was considered as a high causal factor for soil salinity. Moderate and slightly salinity conditions were found in fine loamy and coarse loamy soils, which was defined as a moderate causal factor. Fine silty did not have an effect to soil salinity that classed in a low or non-causal factor.

When topographic elevation map (DEM) was crossed with EC values, the elevation did not show direct relations with EC value. During the field survey discussion with local experts and from farmers interview it was shown that higher salinity zones are located in lower elevated areas. In this case, elevation data in combination with soil texture was related soil salinity. This was verified in the field. The combined data of elevation and soil texture enabled to relate with EC values in both seasons, so all of the soil textures in lower elevation (< 161 m.) areas are given a higher EC value than higher elevation areas. Mainly in fine textured soil with elevation levels less than 159 meters getting the highest EC are categorized as severe salinity. Fine textured soils are normally deposited in lower elevation and this type of soils limits horizontal movement of surface and groundwater. This results to the accumulation of saline water and eventually rises to near surface through capillary rise.

Land use map is one of the parameters used in the model due to the fact that the correlation results of land use and EC value showed a significant criterion for soil salinity mainly in cassava, marsh and swamp and rice paddy/marsh and swamp. Marsh and swamp and rice paddy/marsh and swamp are 2 land use types cultivated in higher EC zones therefore there are considered as a soil salinity indicator.

The last parameter for the salinity model, NDVI was useful, which related to relate crop growth and productions particular rice paddy. Soil salinity directly decreased fertilization of florets in panicle initiation stage and continuously decreased crop yields (Pearson & Bernstein, 1959). When NDVI and EC data had been correlated, the results revealed a negative relationship took place within the correlation between NDVI and EC values. The NDVI values were categorized in 3 classes related to soil salinity as non and low salinity (NDVI > 0.65), moderate and strongly salinity (0.55 < NDVI > 0.65) and severe salinity (NDVI < 0.55).

Table 4-4: Criteria of initial conditioning factors for the soil salinity model

Salinity level	Soil texture	Elevation (m)	Land use	NDVI
Very high	Fine	< 161	ms, rms	< 0.55
			rms	0.65 - 0.55
High	Fine		c, r, sg	< 0.55
			ms, r, sg	0.65 - 0.55
			ms, rms	> 0.65
			ms,r, rms	< 0.55
			rms	0.65 - 0.55
Moderate	Fine	< 161	c	0.65 - 0.55
			c, r, sg	> 0.65

		> 161	c, sg	< 0.55
			ms, r	0.65 - 0.55
			ms,r, rms	> 0.65
	Fine loamy	< 161	ms,r, rms	< 0.55
	Coarse loamy	< 161	ms,r, rms	< 0.55
Low	Fine	> 161	c, sg	0.65 - 0.55
			c, sg	> 0.65
	Fine loamy	< 161	sg	< 0.55
			ms,r, rms, sg	0.65 - 0.55
			ms,r, rms	> 0.65
		> 161	ms,r, rms	< 0.55
	Coarse loamy	< 161	sg	< 0.55
			ms,r, rms, sg	0.65 - 0.55
			ms,r, rms	> 0.65
		> 161	ms,r, rms	< 0.55
	Fine silty	< 161	ms,r, rms, sg	< 0.55
Non	Fine loamy	> 161	c, sg	< 0.55
			c, r, ms, rms, sg	0.65 - 0.55, > 0.65
	Coarse loamy	< 161	sg	> 0.65
		> 161	c, r, ms, rms, sg	0.65 - 0.55, > 0.65
	Fine silty	< 161	c, r, ms, rms, sg	0.65 - 0.55, > 0.65
		> 161	c, r, ms, rms, sg	< 0.55, 0.65 - 0.55, > 0.65

Notes: Land use (c = cassava, r = rice, ms = marsh and swamp, rms = rice paddy/marsh and swamp, sg = scrub/grass)

4.3.2. Generation of a decision tree

Considering the criteria for soil salinity conditioning factors as shown in Table 4-4 a decision tree was made (Figure 4-9). For assessing soil salinity soil texture is the most important indicator, which is followed by elevation, land cover and NDVI respectively. For fine silty soil at higher elevation salinity level is none and at lower elevation areas it is classified as low salinity. For other soil types, susceptibility to soil salinity depends on weight of evidence of conditional factors. Thus, the final assessment was done from the combination of all attributes. Decision rules were applied in decision trees and then the affectability assessment were performed using map overlay procedures in raster-based GIS environment. A decision tree for assessing soil salinity susceptibility of fine textured soil is given in Figure 4-9.

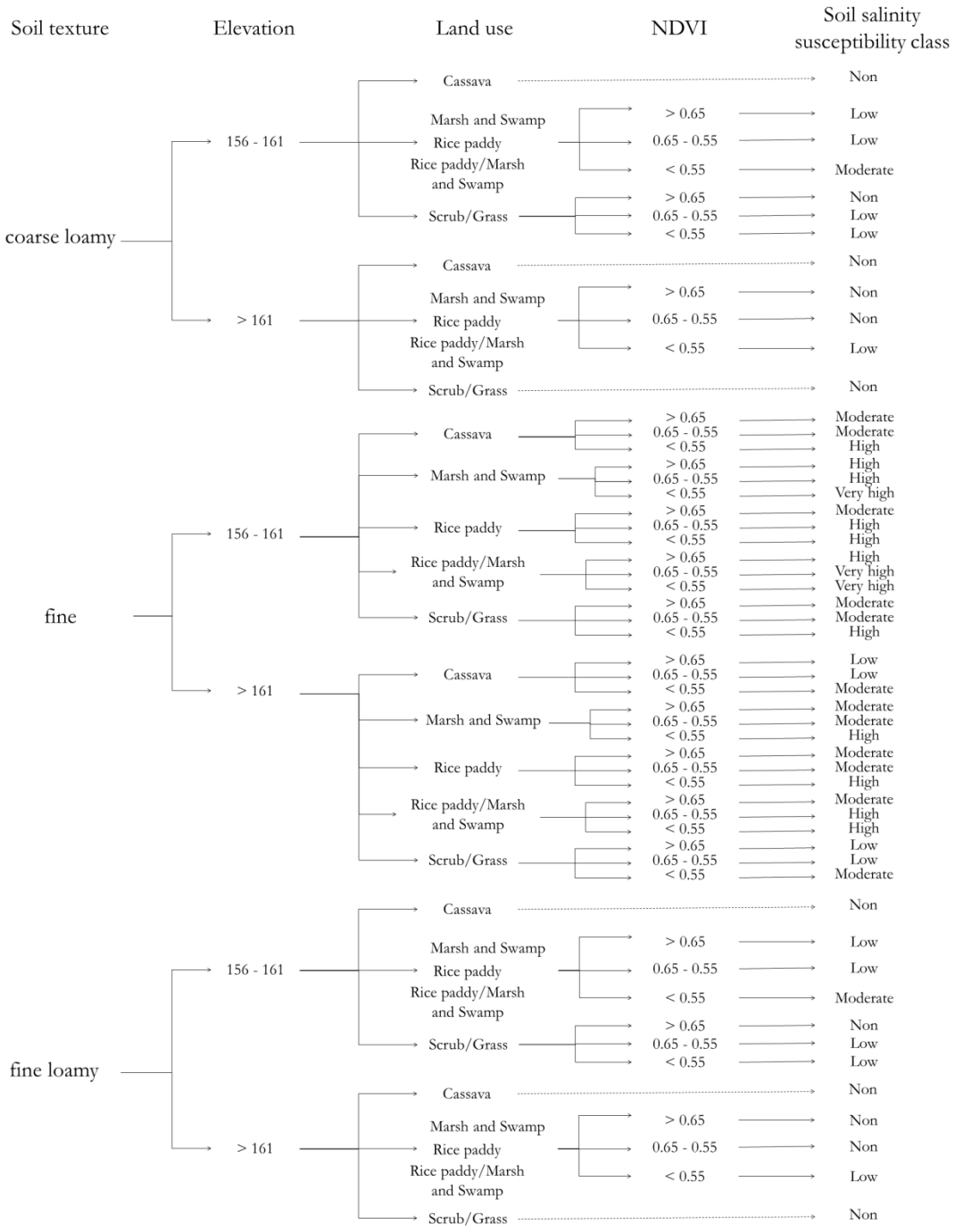

Figure 4-9: Decision tree for accessing the susceptibility at soil salinity

4.3.3. Soil salinity susceptibility assessment

Soil Salinity susceptibility assessment was applied in a raster-based GIS environment which follows the decision rules as shown in the decision trees. It was done using two-dimension table function in ILWIS. Susceptibility assessment results are given in Table 4-5 and Figure 4-10. Nearly half of the study area resulted to be susceptible to slightly saline, moderate saline at 14.30% and strongly saline at 9.06% while only 2.84% was exposed to severe saline. To compare with the salinity map for IDD, the summary areas of very high and high susceptibility were almost similar in 2 data sources at 11.90% (decision tree) and 10.25% (LDD), so non and low susceptibility of soil salinity was to sum up the same numbers as well at 73.80 and 82.28 % respectively.

Table 4-5: Comparative summary of results in terms of area and percentage between Decision Tree and LDD outputs

Susceptible rating	Decision tree		Land Development Department (LDD)	
	Area (km²)	%	Area (km²)	%
non	0.93	18.68	3.30	66.01
low	2.76	55.12	0.81	16.27
moderate	0.72	14.30	0.37	7.47
high	0.45	9.06	0.21	4.28
very high	0.14	2.84	0.30	5.97
Total	5.00	100	5.00	100

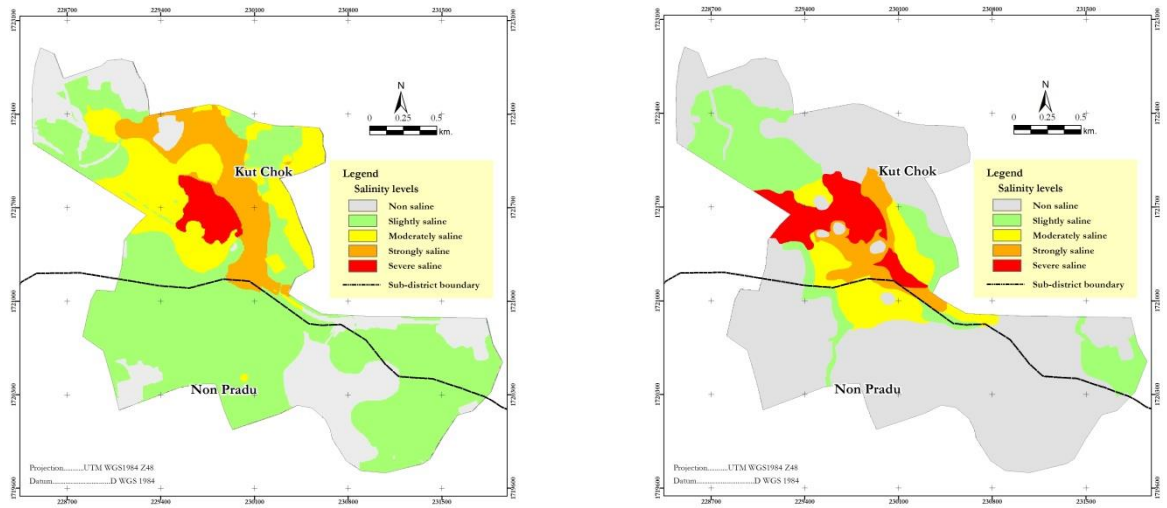

Figure 4-10: Soil salinity susceptibility assessment comparison between decision tree (left) and LDD (right)

4.4. Soil moisture retrieval from Radarsat-2 imagery

4.4.1. Model parameters

To use the model on soil moisture estimation using SAR data proposed by Das & Paul, 2015, the model's parameters have been formulated as shown in Table 4-6

Backscatter coefficients (σ°) relate to a percentage of sand and clay. Moreover, Rougher surfaces generate a larger scattering coefficients response (Ulaby et al., 1979). The backscatter coefficient values range from -18.60 to 2.99 dB with mean of -6.74 (±2.39) for HH polarization and from -25.61 to -9.04 dB with mean of -16.87 (±1.74) for in HV polarization on October 8, 2016

The dielectric constant range from 6.49 to 34.05 with mean value 14.97 (±2.74) in the wet season

Surface roughness (r.m.s.) refers to the effect of the surface and vegetation morphology under natural conditions and it considered as one parameter for SM retrieval by the semi-empirical model (Baghdadi et al., 2004). In this thesis, the surface roughness was calculated using the ratio of HV/HH polarizations, in wet season it ranges between 1.06 to 9.69 with the mean of 2.83 (±1.26).

Table 4-6: Descriptive statistics of main variables for semi-empirical model in dry and wet seasons.

Duration	Variable	Minimum	Maximum	Mean	Std. deviation
Dry season (January 15, 2016)	σ° HH (dB)	-20.49	4.47	-9.16	2.28
	σ° HV (dB)	-28.67	-5.43	-17.86	2.31
	ε	3.12	16.34	7.18	1.32
	r.m.s.	0.98	9.22	2.05	0.61
Wet season (October 8, 2016)	σ° HH (dB)	-18.60	2.99	-6.74	2.39
	σ° HV (dB)	-25.61	-9.04	-16.87	1.74
	ε	6.49	34.05	14.97	2.74
	r.m.s.	1.06	9.69	2.83	1.26

4.4.2. Soil moisture mapping and validation

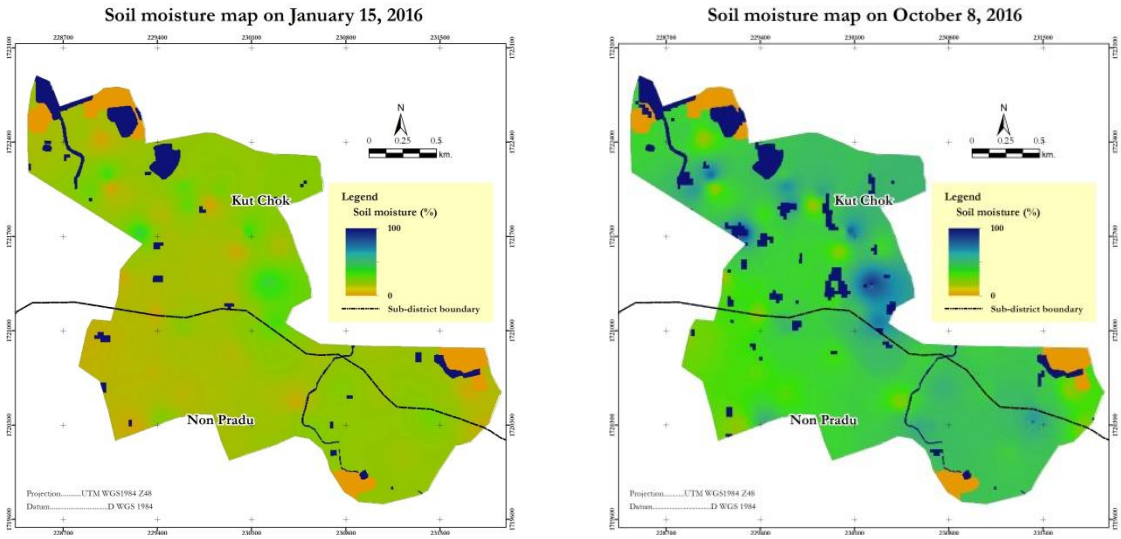

Figure 4-11: The estimated SM map from a Radarsat-2image on dry season(left) and wet season (right).

Table 4-7: Examples of estimated SM in dry and wet seasons.

Duration	Variable	Minimum	Maximum	Mean	Std. deviation
Dry season	SM (%)	4.27	47.57	17.64	4.42
Wet season	SM (%)	15.04	97.65	43.35	9.10

The Radasat-2 image, obtained on 8 October 2016, was processed to generate soil moisture map (Figure 4-11) using the empirical model described by Das & Paul, 2015. For this purpose "modelBuilder" operation in Arc GIS 10.4.1 was used. Statistics of the estimated SM in wet and in dry season are presented in Table 4-7. Since the Radarsat-2 image was taken in the rainy season some areas especially rice fields with standing water were assumed to have 100% SM values. Similarly the water bodies were masked

out. The backscatter signature of water is quit distinctive as compared with other land cover which appears darker in a SAR image(Joyce et al., 2009) In the same way, urban areas were also masked out as non SM areas (0 %).

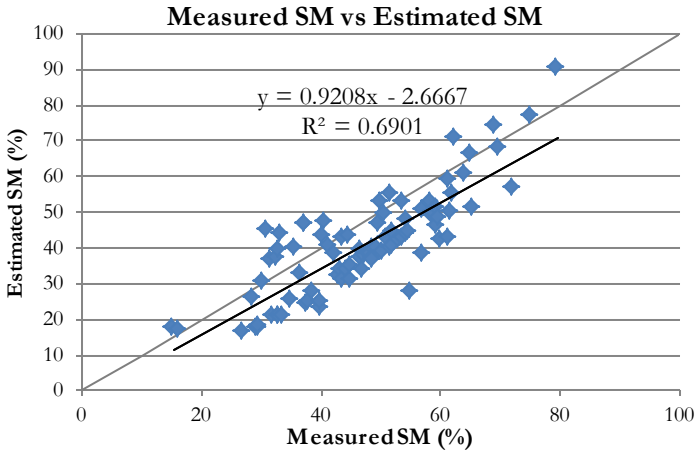

Figure 4-12: The scatter plot of linear regression relationship between measured SM and estimated SM.

To see how good is the soil moisture estimation the measured SM points were plotted against estimated SM (Figure 4-12). Some of the points lied below a slope of one-to-one line that means the estimated SM gave in general lower values than the measured SM. The correlation coefficient is 0.69. It means an uncertainly of about 30 % which come from model parameter or errors in field measurements.

4.4.3. Sensitivity analysis

The surface roughness (r.m.s.) was calculated using the ratio of HV/HH polarization. To see how sensitive this is in SM estimation, the surface roughness was increased by a factor of 20, 40, 60 and 80 percent and corresponding soil moistures were estimated. It shows that the increasing of surface roughness did not have any impact on estimated SM values (Figure 4-13).

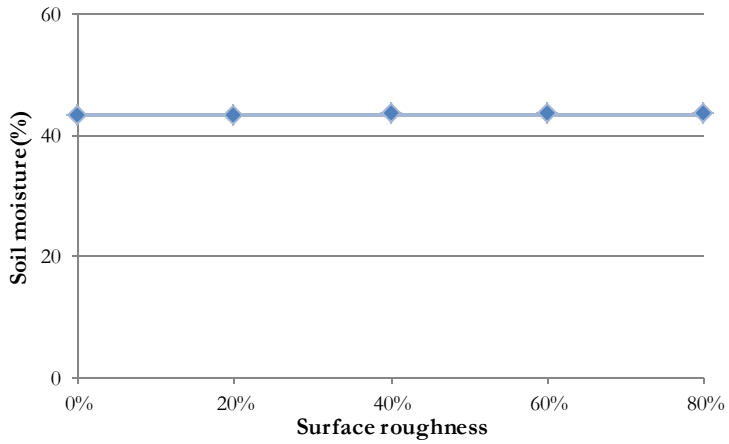

Figure 4-13: Result of sensitivity analysis shows the null effect of surface roughness to soil moisture values.

4.4.4. Temporal soil moisture maps

Monthly SM maps were produced by using the empirical approach as described above with the recalculated model parameters according to the Radarsat-2 imagery from specific month. While some model parameters enable to apply based on backscatter polarizations of each Radarsat-2 image, dielectric

constant calculation required SM content values from field measurement or lab analysis. For this purpose, the Soil Moisture and Ocean Salinity (SMOS) satellite that provided World SM content products in many temporal levels were downloaded and correlated with the average value of SM field and lab interpolation.

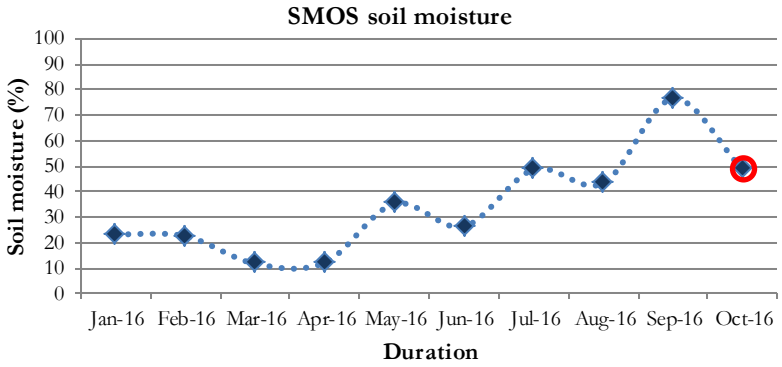

Figure 4-14: Levels of SM content from SMOS data as indicated by the blue dots used to complement measured SM shown in red dot to calculate dielectric constant.

In Figure 4-14, the red circle presented the average value of SM from field and lab interpolation about 49.33 % and SMOS data gave almost the same SM values about 48.64 %. So SM values of SMOS data were suitable for using and calculating different percentages SM on the same day of Radarsat-2 images to compare with the field and lab average value.

The different SM percentages for each date corresponding to Radarsat-2 images were used for calculating dielectric constants after which the empirical model for estimating SM had been executed to generate monthly SM maps as shown in Figure 4-15.

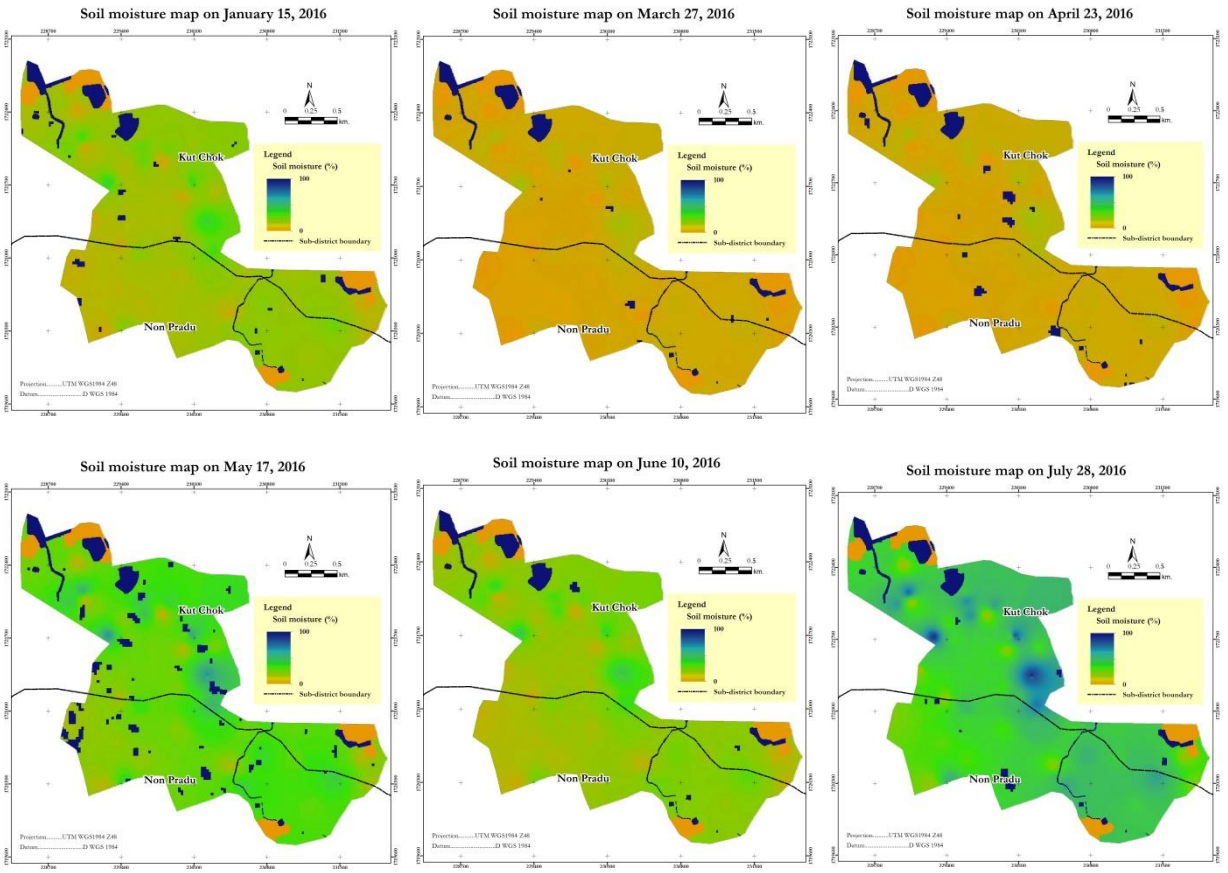

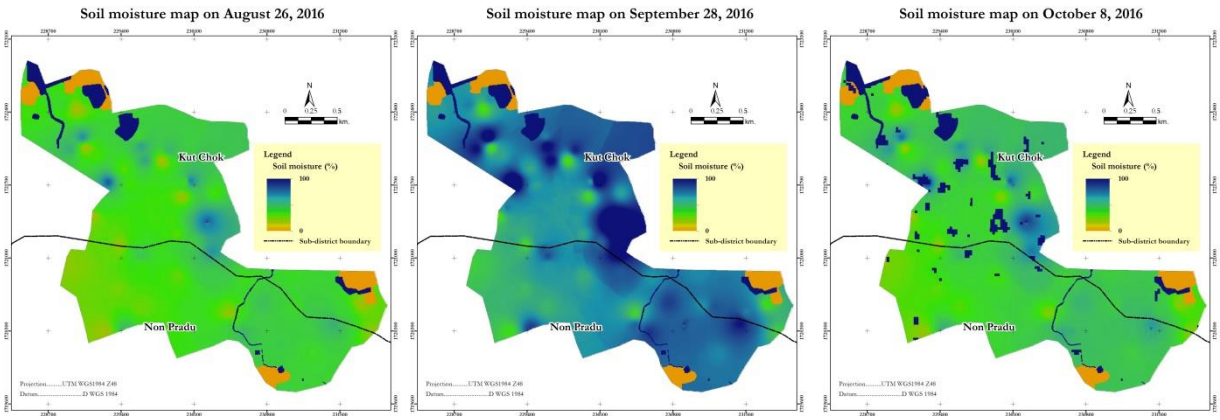

Figure 4-15: Monthly SM maps from January to October, 2016 which illustrates changing of SM levels over the time period. October was a maximum humidity month and March was a minimum humidity month.

Monthly SM maps seem to be reasonable results considering with daily rainfall data (Figure 4-16). The lowest SM with mean value 10 % was on March 27, 2016. The study area had no rain for 68 consecutive days. Rainy period is from May until October, so SM percentages gradually increased from May to October that is illustrated on monthly SM maps, the highest amount of monthly rainfall was recorded in September which is consistent with SM map with mean value 70 % (the highest in the year).

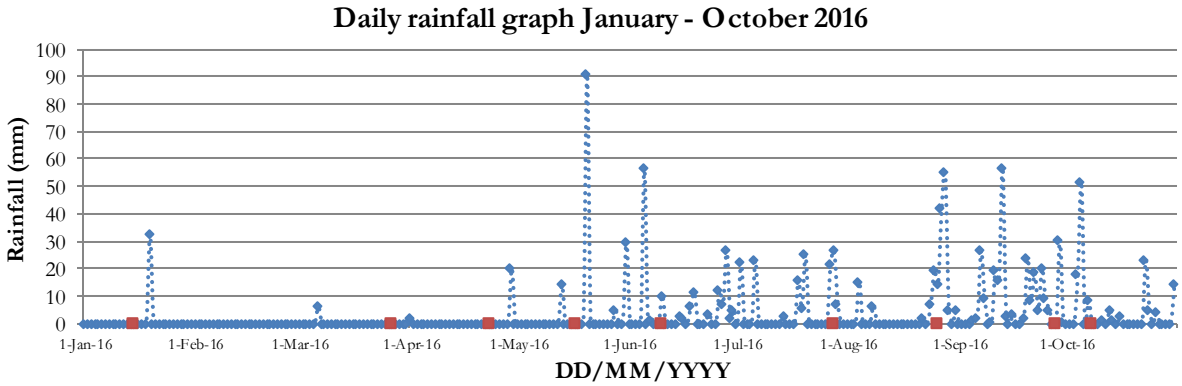

Figure 4-16: Daily rainfall during January to October 2016 overlay with points of exactly date with SM retrieval from radarsat-2 images.

Correlation between EC and soil moisture values from field measurements indicates that periods having low soil moisture (January) have high EC values. Therefore, having established the relationship between the two variables (EC and SM), it can be concluded that the month of March should have the highest level of soil salinity (high EC values) since it has the lowest soil moisture based on rainfall data. As shown in Figure 4-16 about two months of consecutive dryer period exist in March.

4.5. Results of long-term climatic data

4.5.1. Monthly rainfall data

In Bua Yai area, the average yearly rainfall over 29 years is 998 m, it is lower than the average yearly rainfall all of Thailand (1,587 mm.). The rainy season starts in May and ends in October. During rainy season, the average total monthly rainfall ranges from 108.2 to 185.7 mm. The rest of the year is virtually dry with less than 50 mm. per month.

In 2016, the amount of monthly rainfall is higher than the long term average for every month of rainy season. For dry season, there are lower amounts than the average monthly rainfall in February to April, while there is higher amount only in January (Figure4-17).

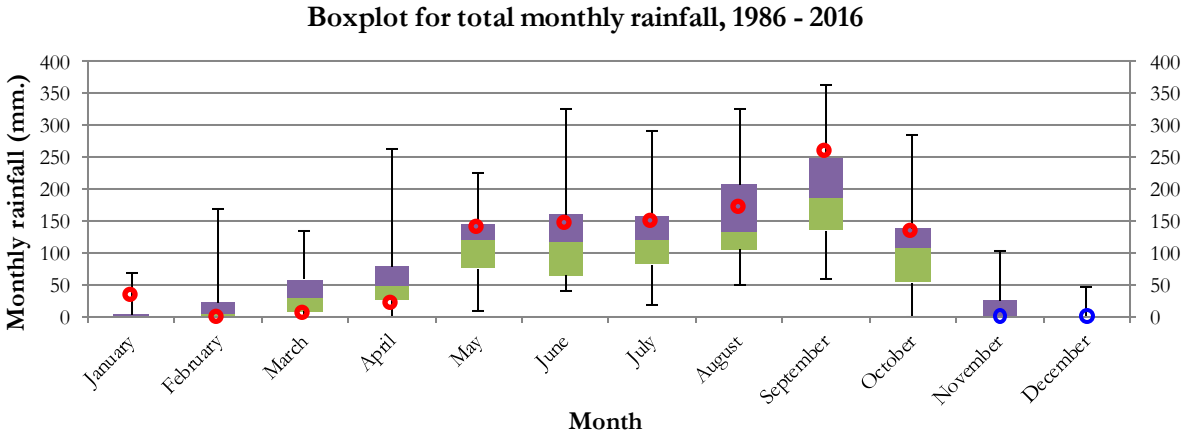

Figure 4-17: Boxplot of total monthly rainfall during 1986 – 2016, bottom and top of boxes are the lower and upper quartiles and band near middle of boxes is the median. Blue and Red circles pointed total monthly rainfall in 2015 and 2016 respectively.

4.5.2. Standardized Precipitation Index (SPI)

3 month SPI

The 3-month SPI was calculated with moving values over 3 months between March, 1986 to October, 2016. The overall results shows SPI values had a lowest position at -2.24 (extremely dry) in April 2013 and a highest position was pointed at 2.47 (extremely wet) in February 2000. These results corresponded to a high value of total loss from drought about 75 million euro in 2013 which was recorded by Department of Disaster Prevention and Mitigation, (2013) For 2016, the lowest value of negative SPI reached -1.32 (moderate dry) in April and the highest values of positive SPI peaked at 0.79 in September (Figure 4-18). The precipitation anomaly occurred during February to April that reflected a decrease of soil moisture level in that time as well.

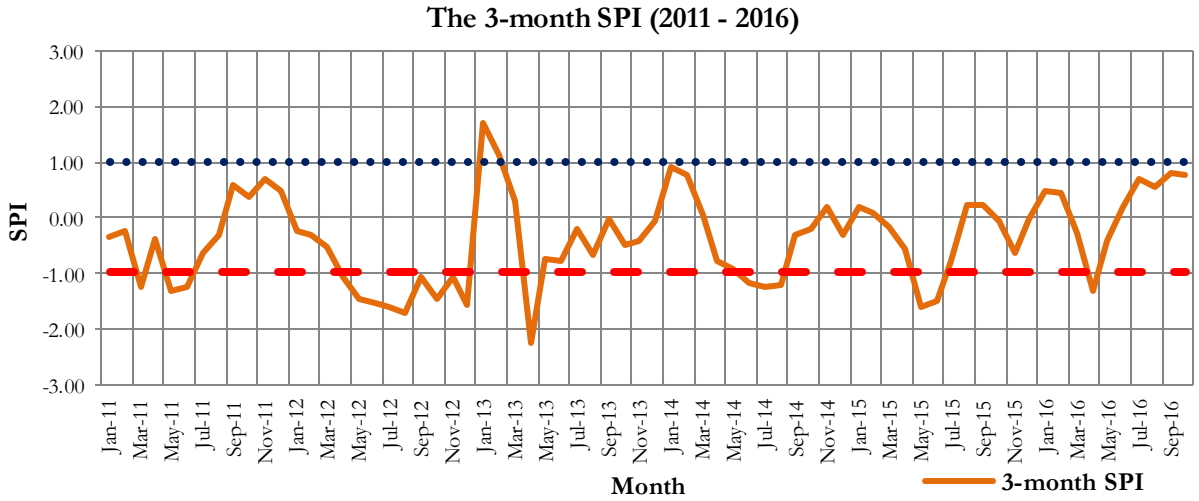

Figure 4-18: The 3-month SPI for every month between 2011 and 2016. The horizontal dot and dashed line specify the thresholds between wet and dry year.

6 month SPI

The 6-month SPI was also calculated using moving values over 6 months over the same period. The results shows SPI values had a lowest position at -1.83 (severely dry) in August 2012 and a highest position was pointed at 2.71 (Extremely wet) in May 2000. For 2016, the lowest values of negative SPI also reached at -1.04 in April and the highest values of positive SPI peaked at 0.83 in October (Figure 4-19) which is considered within the normal range. The precipitation pattern did not have more an influence on a changing of ground water level.

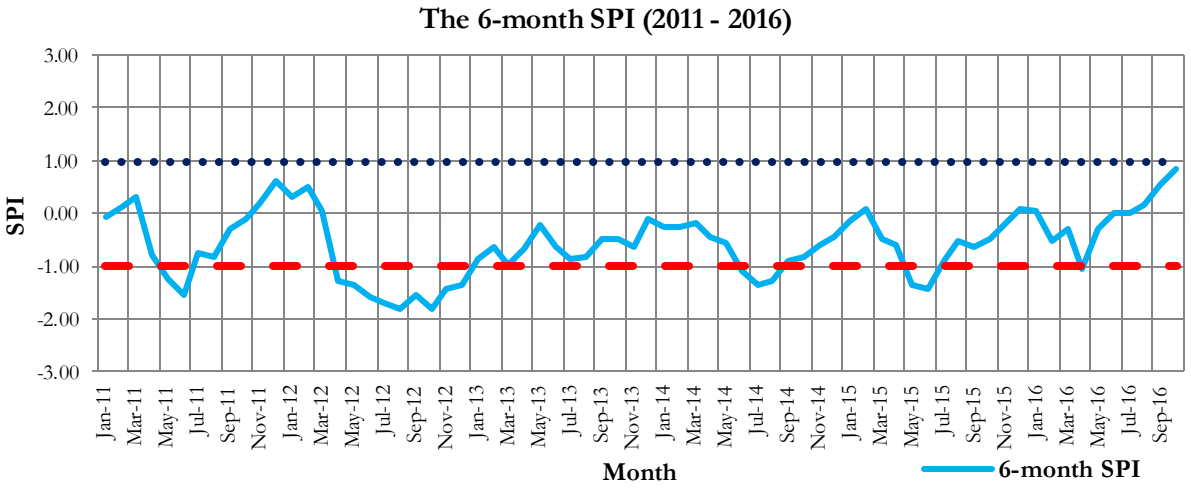

Figure 4-19: The 6-month SPI for every month between 2011 and 2016. The horizontal dot and dashed line specify the thresholds between wet and dry year.

As compared to other years the situation in 2016 seems to be normal (no drought) as shown by 3 and 6 months SPI results having in general positive values (Figure 4-20). Severe and extremely dry years are in 2004, 2010 and in 2013 when the SPI values were below zero at 1-.95, -2.09 and -2.24 respectively (Figure 4-20). The 3 month SPI is related to SM. In 2016 the 3 month SPI showed dryness from January until April and then it continuously increased from May to October. While 6 month SPI reflects a slower processing variable as groundwater recharges, the 6 month SPI values showed a same movement with a narrow change mean, that groundwater had higher level than April but lower level than October as well.

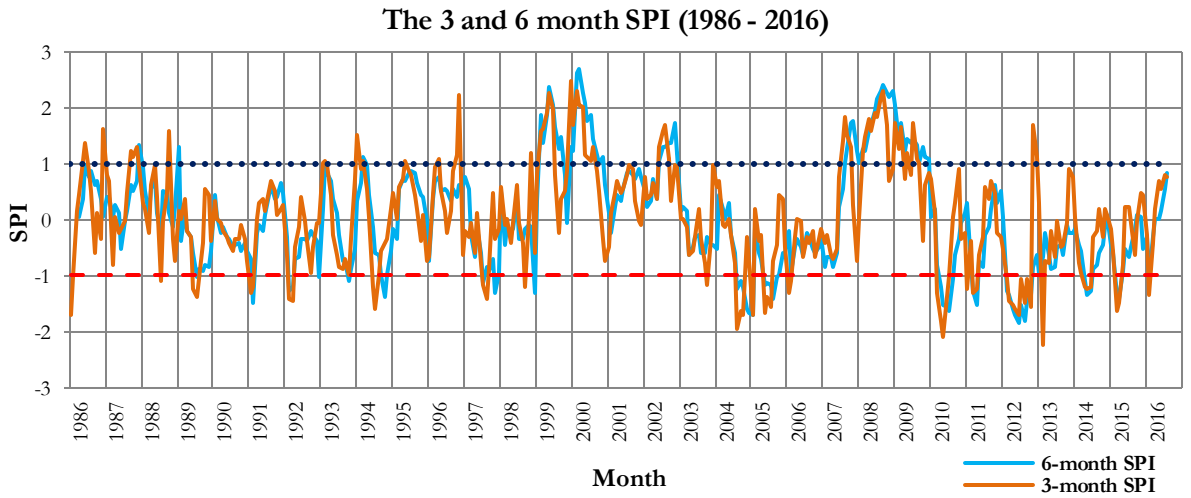

Figure 4-20: 3 and 6 month SPI for every month over 30 year

Based on the SPI results in 2016, the month of January shows lower SPI values which denote a dryer period as compared to October. This can be related to the measured rainfall data of the same year. Records show that from the period October 10, 2015 to January 19, 2016, only one rainfall event occurred, resulting to a dryer condition. On the other hand, October records show that rainfall occurred almost every day which leads to a wetter condition. The meteorological situations on both months (January and October) influence the soil moisture (SM) and groundwater condition in the area which has a negative relation with EC values as discussed in chapter 4.2.1. Moreover, EC values are directly related with soil salinity.

Low SPI suggests high EC values meaning high salinity level in the soil (January) which is considered dry season. In contrast, SPI values in October are higher which is related to lower EC or low salinity level. This is attributed to high soil moisture content, having influence in lowering the salinity level during the wet season.

Likewise, SPI can be correlated with rice production data covering the period 2011 – 2016 acquired from Department of Agriculture Extension (DOAE). It shows that the trend of rice produced in a certain year is associated with the SPI level on the same year. Generally, the cultivation period in the study area is undertaken on months with high SPI values resulting to high crop production. Crop production data for paddy rice was available for the period 2011 – 2015. It shows highest crop production in 2011 (2.64 ton/hectare) (Table 4-8). The SPI value range during July to December was -0.64 to 0.71. While the lowest crop production is in 2012 with SPI range -1.7 to -1.05. According to Srisuphaolarn (2016) the suitable period for rice cultivation is between late April and mid-November because of available moisture for growing field crops.

Table 4-8: Annual rice production obtained from Department of Agriculture Extension (DOAE).

Year		2011	2012	2013	2014	2015	2016
the annual production	Bua Yai	2.64	2.26	2.36	2.14	2.15	-
(ton/hectare)	Sida	2.74	2.07	2.25	2.16	2.16	

5. CONCLUSIONS

5.1. Conclusion

In this research, soil salinity susceptibility assessment is crucial for land use planning especially land parcel reformation. Soil salinity is frequently affected by more than conditional factors simultaneously, the modelling of which was time-consuming task. Although spatial models were achieved with good results, insufficient data available is often as a barrier to application enhancement in many developing countries. Moreover, applicable models very few existed for soil salinity, modelling by decision trees provided an alternative solution for soil salinity susceptibility assessment in such condition. A decision tree was simply to construct, the decision rules can be found by implementing GIS map overlay functions. This technique utilized the correlation results of conditional factors for soil salinity (increase of EC of soil) prioritizing the factors reliable for soil salinity assessment. The model is flexible and can be modified to suit different drought conditions.

In the following section the answers for initially designed research questions are briefly described:

1. *How is (degree of) salinity illustrated/ exemplified in vegetation types, elevation, soil properties and soil moisture?*

Among many soil salinity indicators the study shows that soil texture is the main conditional factor in soil salinization process in the study area. Soil salinity is generally found in fine textured soil. After soil texture, the second important indicator seems to be terrain elevation, the low lying areas are more prone to soil salinity because of closeness to groundwater. Finally, the last factor is NDVI which is inversely related to soil salinity e.g. high NDVI means low salinity. The 4 main conditional factors for soil salinity assessment are soil texture, elevation, land use and NDVI.

2. *Does the spatial model represent the soil salinity scenario of the study area?*

This Spatial model was applicable to assess soil salinity for currently available data with effective correlations to EC measurements. Spatial model based on 4 main conditional factors by using the decision tree which classifying soil salinity susceptibility maps into 5 classes. Very high class located in the middle area of 0.14 km^2 and non and low classes cover more than 73 % of total area with 0.93 and 2.76 km^2 respectively. The rest in moderate and high classes distributed over the upper part at 0.72 and 0.45 km^2.

3. *What is the extent of salinity distribution in different season?*

The salinity map in the dry season from Land Development Department (LDD) shows the problem mostly in the middle part of the study area. LDD assumed the capillary force in each soil texture class, soil salinity level is differentiated by rising of saline groundwater which coincided with low elevated areas (closer distance to groundwater). For wet season, the salinity assessment was carried out using 4 main parameters. In addition to the above 2 reasons, the agricultural activities especially rice paddy cultivation affects salinity distribution. For growing rice farmers manage the land in such a way that there is enough standing water in the field, this helps in the transportation of the saline water to low lying areas. Therefore the salinity extent in wet season is wider than in dry season, the difference of which is about 2.37 km^2 (47%).

4. *Does soil moisture generated from Synthetic aperture radars (SAR) image coincide with the ground truth data?*

Soil moisture retrieval from applying a semi-empirical model on SAR data with 3 model parameters namely backscatter coefficients, dielectric constant and surface roughness, had a good correlation with measured soil moistures. The model has an $R^2 = 0.69$ of estimated versus measured soil moisture value.

5. *How can drought index be used to soil salinity conditions in the area?*

Standardized Precipitation Index (SPI) was applied to determine drought conditions in the area which is based on 30 year rainfall data. In 2016, the moving average of 3 month SPI have drought index results

ranging from -1.32 to 0.79 and that of 6 months SPI from -1.04 to 0.83. Both the SPI index results fall within the classes moderately dry (-1.00 to -1.49) to normal (-0.99 to + 0.99) which means that 2016 can be considered to have near normal situation. While SPI has a lowest values at 2.24 in 2013 as extremely dry year, the result is conform with high total loss in the same year about 75 million euro. The EC measurements in January and October can be represented soil salinity levels because the results of 6 month SPI revealed that groundwater continuous influenced on saline water movement.

6. *How soil salinity affects the crop stage and production?*

On October, rice paddy fields were mainly in a flowering stage, the measured NDVI value ranging from 0.6 – 0.7. Soil salinity affects the flowering stage of rice as mentioned in many studie, and the correlation results between EC versus NDVI shows that high and very high salinity related to NDVI values lower than 0.56. Analysis of crop productions in relation to SPI during 2011 – 2015 shows that highest crop production at 2.64 ton/hectare is associated with a high SPI value range (-0.64 to 0.71) which is classified as being normal year meaning that sufficient moisture was available for plant growth in 2011. When there is sufficient rain it lower soil salinity problem. While the lowest crop production is in 2012 with SPI range -1.7 to -1.05.

5.2. Limitation of this resreach

- The field work period in wet season is not very suitable for data collection especially for collecting soil samples.
- The groundwater level is considered to be constant in this study because of limited data and data distribution.
- The long-term climatic data at Bua Yai station has only rainfall data. Should there be more information such as evapotranspiration, another drought index can be calculated for comparison.

5.3. Future work

- Future students can analyse the spatio-temporal variation of salinity over a series of rains from heavy rainfall to normal year and to drought year to determine change in soil salinity which can directly be attributed to rainfall and to other anthropogenic and natural factor

LIST OF REFERENCES

Aaen, P., Plá, J. A., & Wood, J. (2007). Model Validation. In *Modeling and Characterization of RF and Microwave Power FETs:* (pp. 323–352). Cambridge: Cambridge University Press. https://doi.org/10.1017/CBO9780511541124.010

Abdolrahim, P. (2003). *Analysis of the relationship between soil salinity dynamics and geopedologic properties*. *MSc Thesis*. Faculty of Geo-Information Science and Earth Observation of the University of Twente.

Abramowitz, M., & Stegun, I. A. (1964). *Handbook of Mathematical Functions With Formulas, Graphs, and Mathematical Tables* (1st ed.). Washington, D.C. Retrieved from http://people.math.sfu.ca/~cbm/aands/intro.htm

Anderson, J. R., Hardy, E. E., Roach, J. T., & Witmer, R. E. (1976). A Land Use And Land Cover Classification System For Use With Remote Sensor Data. *Geological Survey Professional Paper A Revision of the Land Use Classification System as Presented in U.S. Geological Survey*.

Ayers, R. S., & Westcot, D. W. (1985). *Water quality for agriculture*. Food and Agriculture Organization of the United Nations.

AZLAN, A., WENG, A., IBRAHIM, C. ., & NOORHAIDAH, A. (2012). Correlation between Soil Organic Matter, Total Organic Matter and Water Content with Climate and Depths of Soil at Different Land use in. *J. Appl. Sci. Environ. Manage. Dec*, *16*(4), 353–358. Retrieved from www.ajol.info

Baghalian, K., Haghiry, A., Naghavi, M. R., & Mohammadi, A. (2008). Effect of saline irrigation water on agronomical and phytochemical characters of chamomile (Matricaria recutita L.). *Scientia Horticulturae*, *116*(4), 437–441. https://doi.org/10.1016/j.scienta.2008.02.014

Baghdadi, N., Gherboudj, I., Zribi, M., Sahebi, M., King, C., & Bonn, F. (2004). Semi-empirical calibration of the IEM backscattering model using radar images and moisture and roughness field measurements. *International Journal of Remote Sensing*, *25*(18), 3593–3623. https://doi.org/10.1080/01431160310001654392

Belal, A.-A., El-Ramady, H. R., Mohamed, E. S., & Saleh, A. M. (2014). Drought risk assessment using remote sensing and GIS techniques. *Arabian Journal of Geosciences*, *7*(1), 35–53. https://doi.org/10.1007/s12517-012-0707-2

Bobby, R., Mark Alley, W. G., Holshouser, D., & Thomason, W. (2009). Precision Farming Tools: Soil Electrical Conductivity. *Virginia Cooperative Extension*, *442–508*.

Brisco, B., Touzi, R., van der Sanden, J. J., Charbonneau, F., Pultz, T. J., & D'Iorio, M. (2008). Water resource applications with RADARSAT-2 – a preview. *International Journal of Digital Earth*, *1*(1), 130–147. https://doi.org/10.1080/17538940701782577

Clermont-Dauphin, C., Suwannang, N., Grünberger, O., Hammecker, C., & Maeght, J. L. (2010). Yield of rice under water and soil salinity risks in farmers' fields in northeast Thailand. *Field Crops Research*, *118*(3), 289–296. https://doi.org/10.1016/j.fcr.2010.06.009

Das, K., & Paul, P. K. (2015). Soil moisture retrieval model by using RISAT-1, C-band data in tropical dry and sub-humid zone of Bankura district of India. *The Egyptian Journal of Remote Sensing and Space Science*, *18*(2), 297–310. https://doi.org/10.1016/j.ejrs.2015.09.004

Delta-T Devices Ltd. (2007). User Manual for the WET Sensor type WET-2. Retrieved December 6, 2016, from http://www.delta-t.co.uk/product/wet-2-horticulture/

Department of Disaster Prevention and Mitigation. (2013). Retrieved February 11, 2017, from http://122.155.1.145/cmsdetail.directing-6.191/10039/menu_4469/2015.1/สถิติสาธารณภัย+ปี+2556

Department of Environment, Q., & Management, R. (2011). *Salinity management handbook* (2nd ed.). Queensland. Retrieved from https://publications.qld.gov.au/storage/f/2013-12-19T04%3A10%3A23.754Z/salinity-management-handbook.pdf

Department of Mineral Resources. (1999). Geological Map of Thailand, Scale 1:1,000,000. Retrieved from http://www.dmr.go.th/more_news.php?cid=187&filename=index

Department of Transportation. (1998). *METHOD OF TEST FOR PERMEABILITY OF SOILS*.

Diacono, M., & Montemurro, F. (2015). Effectiveness of Organic Wastes as Fertilizers and Amendments in Salt-Affected Soils. *Agriculture*, *5*(2), 221–230. https://doi.org/10.3390/agriculture5020221

Dubois, P. C., van Zyl, J., & Engman, T. (1995). Measuring soil moisture with imaging radars. *IEEE Transactions on Geoscience and Remote Sensing*, *33*(4), 915–926. https://doi.org/10.1109/36.406677

Dunkel, Z. (2009). Brief surveying and discussing of drought indices used in agricultural meteorology. *Quarterly Journal of the Hungarian Meteorological Service*, *113*(1–2), 23–37.

FAO. (2006). 6. Soil Texture. Retrieved January 30, 2017, from ftp://ftp.fao.org/fi/cdrom/fao_training/fao_training/general/x6706e/x6706e06.htm

FAO. (2014). Understanding the drought impact of El Niño on the global agricultural areas: An assessment using FAO's Agricultural Stress Index (ASI).

FAO. (2016). *AquaCrop training handbooks Book I Understanding AquaCrop*. Rome. Retrieved from http://www.fao.org/3/a-i6051e.pdf

Feller, C., & Beare, M. H. (1997). Physical control of soil organic matter dynamics in the tropics. *Geoderma*, *79*(1–4), 69–116. https://doi.org/10.1016/S0016-7061(97)00039-6

Fetter, C. W. (1994). *Applied Hydrogeology* (Third). New Jersey: University of Wisconsin-Oshkosh, Prentice Hall, New Jersey. Retrieved from https://www.amazon.com/Applied-Hydrogeology-4th-C-W-Fetter/dp/0130882399

Food and Agriculture Organization of the United Nations. Soil Resources, D. and C. S. (1976). *Prognosis of salinity and alkalinity : report of an expert consultation, Rome, 3-6 June 1975*. Food and Agriculture Organization of the United Nations.

Gardner, L. S., Hamworth, H. ., & Na Chiengmai, P. (1967). *Salt resources in Thailand*. Bangkok: Department of Mineral Resources.

Ghassemi, F. (Fereidoun), Jakeman, A. J. (Anthony J., & Nix, H. A. (Henry A. (1995). *Salinisation of land and water resources : human causes, extent, management, and case studies* (Australian). Sydney, N.S.W., : NSW University Press.

Guttman, N. B. (1998). COMPARING THE PALMER DROUGHT INDEX AND THE STANDARDIZED PRECIPITATION INDEX. *Journal of the American Water Resources Association*, *34*(1), 113–121. https://doi.org/10.1111/j.1752-1688.1998.tb05964.x

Hall, N., Greiner, R., & Yongvanit, S. (2004). Adapting modelling systems for salinity management of farms and catchments in Australia and Thailand. *Mathematics and Computers in Simulation*, *64*(3), 319–327. https://doi.org/10.1016/S0378-4754(03)00098-3

Hallikainen, M., Ulaby, F., Dobson, M., El-rayes, M., & Wu, L. (1985). Microwave Dielectric Behavior of Wet Soil-Part 1: Empirical Models and Experimental Observations. *IEEE Transactions on Geoscience and Remote Sensing*, *GE-23*(1), 25–34. https://doi.org/10.1109/TGRS.1985.289497

Hao, Z., & AghaKouchak, A. (2013). Multivariate Standardized Drought Index: A parametric multi-index model. *Advances in Water Resources*, *57*, 12–18. https://doi.org/10.1016/j.advwatres.2013.03.009

Haron, M., & Dragovich, D. (2010). Climatic influences on dryland salinity in central west New South Wales, Australia. *Journal of Arid Environments*, *74*(10), 1216–1224. https://doi.org/10.1016/j.jaridenv.2010.04.014

Hayes, M. J., Svoboda, M. D., Wardlow, B. D., Anderson, M. C., & Kogan, F. (2012). Drought Monitoring: Historical and Current Perspectives (pp. 1–19). Retrieved from http://digitalcommons.unl.edu/droughtfacpub

Heim, R. R. (2002). A Review of Twentieth-Century Drought Indices Used in the United States. *Bulletin of the American Meteorological Society*, *83*(8), 1149–1165. https://doi.org/10.1175/1520-0477(2002)083<1149:AROTDI>2.3.CO;2

Heiri, O., Lotter, A. F., & Lemcke, G. (2001). Loss on ignition as a method for estimating organic and carbonate content in sediments: reproducibility and comparability of results. *Journal of Paleolimnology*, *25*, 101–110.

Hills, R. G., & Trucano, T. G. (1999). Statistical Validation of Engineering and Scientific Models: Background.

Hunt, N., & Gilkes, B. (1992). Water erosion. In *Farm Monitoring Handbook* (p. 28). The University of Western Australia: Nedlands. Retrieved from http://sustainableagriculture.perthregionnrm.com/sites/default/files/FMHch5_1.pdf

IPCC. (2012). Managing the Risks of Extreme Events and Disasters to Advance Climate Change Adaptation (SREX). Retrieved from https://www.ipcc.ch/report/srex/

ITC Corebook. (2013). *ITC Corebook*. Enschede: The Faculty of Geo-Information Science and Earth Observation (ITC) of the University of Twente. Retrieved from https://issuu.com/itc-utwente/docs/corebook2013_04_sensors

Jacobs, T., Swinnen, E., & C. Toté, P. (2016). GIO-GL Lot 1, GMES Initial Operations Gio Global Land Component -Lot I " Operation of the Global Land Component " Framework Service Contract N° 388533 (JRC).

Jeong, S., Yu, I., Felix, M. L. A., Kim, S., & Oh, K. (2014). Drought assessment for real-time hydrologic drought index of the Nakdong River Basin in Korea. *Desalination and Water Treatment*, *52*(13–15),

2826–2832. https://doi.org/10.1080/19443994.2013.870713
Joyce, K. E., Belliss, S. E., Samsonov, S. V, Mcneill, S. J., & Glassey, P. J. (2009). A review of the status of satellite remote sensing and image processing techniques for mapping natural hazards and disasters. *Progress in Physical Geography*, *33*(2), 183–207. https://doi.org/10.1177/0309133309339563
Kotb, T. H. S., Watanabe, T., Ogino, Y., & Tanji, K. K. (2000). Soil salinization in the Nile Delta and related policy issues in Egypt. *Agricultural Water Management*, *43*, 239–261.
Land development department. (2009). *Management of saline soil problem in Thailand*. Retrieved from http://www.ldd.go.th/Lddwebsite/web_ord/Technical/pdf/P_Technical03001_5.pdf
LDD. (2010). คู่มือการปฏิบัติงาน กระบวนการบริการแผนที่และข้อมูลแผนที่.
Loffler, E., Thompson, W. P., & Liengsakul, M. (1984). Quaternary geomorphological development of the lower Mun River Basin, North East Thailand. *CATENA*, *11*(4), 321–330. https://doi.org/10.1016/0341-8162(84)90030-4
Lund, E. D., Christy, C. D., & Drummond, P. E. (1999). PRACTICAL APPLICATIONS OF SOIL ELECTRICAL CONDUCTIVITY MAPPING BACKGROUND…THE OPPORTUNITIES AND CHALLENGES OF PRECISION FARMING. *The Proceedings of the 2nd European Conference on Precision Agriculture*.
Mapraneat, V. (2014). Drought conditions and management strategies in Thailand. Retrieved January 28, 2017, from http://www.droughtmanagement.info/literature/UNW-DPC_NDMP_Country_Report_Thailand_2014.pdf
Mccauley, A. (2009). Soil pH and Organic Matter.
Mckee, T. B., Doesken, N. J., & Kleist, J. (1993). THE RELATIONSHIP OF DROUGHT FREQUENCY AND DURATION TO TIME SCALES. *Eighth Conference on Applied Climatology*, 17–22.
Mcnairn, H., Merzouki, A., & Pacheco, A. (2010). ESTIMATING SURFACE SOIL MOISTURE USING RADARSAT-2. *International Archives of the Photogrammetry, Remote Sensing and Spatial Information Science*, *38*.
McNairn, H., Merzouki, A., Pacheco, A., & Fitzmaurice, J. (2012). Monitoring Soil Moisture to Support Risk Reduction for the Agriculture Sector Using RADARSAT-2. *IEEE Journal of Selected Topics in Applied Earth Observations and Remote Sensing*, *5*(3), 824–834. https://doi.org/10.1109/JSTARS.2012.2192416
Metternicht, G. ., & Zinck, J. . (2003). Remote sensing of soil salinity: potentials and constraints. *Remote Sensing of Environment*, *85*(1), 1–20. https://doi.org/10.1016/S0034-4257(02)00188-8
Mishra, A. K., & Singh, V. P. (2011). Drought modeling - A review. *Journal of Hydrology*, *403*(1–2), 157–175. https://doi.org/10.1016/j.jhydrol.2011.03.049
Moran, M. S., Peters-Lidard, C. D., Watts, J. M., Mcelroy, S., Moran, M. S., & Watts, J. M. (2004). Estimating soil moisture at the watershed scale with satellite-based radar and land surface models. *Can. J. Remote Sensing*, *30*(5), 805–826.
Morgan, K., & Jankowski, J. (2004). Saline groundwater seepage zones and their impact on soil and water resources in the Spicers Creek catchment, central west, New South Wales, Australia. *Environmental Geology*, *46*(2), 273–285. https://doi.org/10.1007/s00254-004-0977-4
Murthy, S. K., Kasif, S., & Salzberg, S. (1994). A System for Induction of Oblique Decision Trees. *Journal of Artiicial Intelligence Research Submitted*, *2*(4494), 1–32.
Naresh Kumar, M., Murthy, C. S., Sai, M. V. R. S., & Roy, P. S. (2015). On the use of Standardized Precipitation Index (SPI) for drought intensity assessment.
National Weather Service. (2016). Weather Glossary: D's. Retrieved December 13, 2016, from http://www.srh.weather.gov/srh/jetstream/append/glossary_d.html
NEST 5.1 User Manual. (2014). Retrieved from https://earth.esa.int/web/nest/documents
Nimmo, J. (2013). Porosity and Pore Size Distribution. *Earth Systems and Environmental Sciences*. https://doi.org/10.1016/B978-0-12-409548-9.05265-9
NRCS. (2014). *Soil Electrical Conductivity-Soil Quality Kit* (Guides for Educators). Retrieved from https://www.nrcs.usda.gov/Internet/FSE_DOCUMENTS/nrcs142p2_053280.pdf
Oh, Y., Sarabandi, K., & Ulaby, F. T. (1992). An empirical model and an inversion technique for radar scattering from bare soil surfaces. *IEEE Transactions on Geoscience and Remote Sensing*, *30*(2), 370–381. https://doi.org/10.1109/36.134086
Pearson, G. A., & Bernstein, L. (1959). Salinity Effects at Several Growth Stages of Rice1. *Agronomy Journal*, *51*(11), 654. https://doi.org/10.2134/agronj1959.00021962005100110007x
Peñuelas, J., Isla, R., Filella, I., & Araus, J. L. (1997). Visible and Near-Infrared Reflectance Assessment of

Salinity Effects on Barley. *Crop Science*, *37*(1), 198. https://doi.org/10.2135/cropsci1997.0011183X003700010033x

Pitman, M. G., & Läuchli, A. (2002). Global Impact of Salinity and Agricultural Ecosystems. In *Salinity: Environment - Plants - Molecules* (pp. 3–20). Dordrecht: Kluwer Academic Publishers. https://doi.org/10.1007/0-306-48155-3_1

Quantin, C., Grunberger, O., Suvannang, N., & Bourdon, E. (2008). Land Management Effects on Biogeochemical Functioning of Salt-Affected Paddy Soils. *Pedosphere*, *18*(2), 183–194. https://doi.org/10.1016/S1002-0160(08)60006-5

RADARSAT-2. (2016). Retrieved December 2, 2016, from http://mdacorporation.com/geospatial/international/satellites/RADARSAT-2

RID. (2015). Water Watch and Monitoring System for Warning Center. Retrieved from http://wmsc.rid.go.th/

Rycroft, D. W., Amer, M. H., & Food and Agriculture Organization of the United Nations. (1995). *Prospects for the drainage of clay soils*. Food and Agriculture Organization of the United Nations.

Safavian, S. R., & Landgrebe, D. (1991). A survey of decision tree classifier methodology. *IEEE Transactions on Systems, Man, and Cybernetics*, *21*(3), 660–674. https://doi.org/10.1109/21.97458

Saleh, A. (1993). Soil roughness measurement: Chain method. *Journal of Soil and Water Conservation*, *48*(6), 527–529.

Sánchez, J. M. (2008). *Droughts : causes, effects and predictions*. Hauppauge: Nova Science Publishers. Retrieved from http://cataleg.upc.edu/record=b1344959~S1*cat

Seeboonruang, U. (2013a). Relationship between groundwater properties and soil salinity at the Lower Nam Kam River Basin in Thailand. *Environmental Earth Sciences*, *69*(6), 1803–1812. https://doi.org/10.1007/s12665-012-2012-5

Seeboonruang, U. (2013b). Relationship between groundwater properties and soil salinity at the Lower Nam Kam River Basin in Thailand. *Environmental Earth Sciences*, *69*(6), 1803–1812. https://doi.org/10.1007/s12665-012-2012-5

Şenaut, Z. (2015). *Applied drought modeling, prediction, and mitigation*. Elsevier.

Shahid, S. A. (2013). Developments in Soil Salinity Assessment, Modeling, Mapping, and Monitoring from Regional to Submicroscopic Scales. In *Developments in Soil Salinity Assessment and Reclamation* (pp. 3–43). Dordrecht: Springer Netherlands. https://doi.org/10.1007/978-94-007-5684-7_1

Sheffield, J., & Wood, E. F. (2011). *Drought: Past Problems and Future Scenarios*. Florence: Taylor and Francis. https://doi.org/10.4324/9781849775250

Shi, J., Du, Y., Du, J., Jiang, L., Chai, L., Mao, K., … Wang, Y. (2012). Progresses on microwave remote sensing of land surface parameters. *Science China Earth Sciences*, *55*(7), 1052–1078. https://doi.org/10.1007/s11430-012-4444-x

Shrestha, D. ., Zinck, J. ., & Van Ranst, E. (2004). Modelling land degradation in the Nepalese Himalaya. *CATENA*, *57*(2), 135–156. https://doi.org/10.1016/j.catena.2003.11.003

Soil Quality. (2017). Bulk Density - Measurement. Retrieved January 30, 2017, from http://www.soilquality.org.au/factsheets/bulk-density-measurement

Srinivasa Rao, S., Dinesh kumar, S., Das, S. N., Nagaraju, M. S. S., Venugopal, M. V., Rajankar, P., … Sharma, J. R. (2013). Modified Dubois Model for Estimating Soil Moisture with Dual Polarized SAR Data. *Journal of the Indian Society of Remote Sensing*, *41*(4), 865–872. https://doi.org/10.1007/s12524-013-0274-3

Srisuphaolarn, A. (2016). *Soil characteristics in saline soil areas of salt tolerance trees planting project in Tung Samrit / Lam Sataet areas , Nakhon Ratchasima Province*. Nakhon Ratchasima.

Srivastava, H. S., Patel, P., Navalgund, R. R., & Sharma, Y. (2008). Retrieval of surface roughness using multi-polarized Envisat-1 ASAR data. *Geocarto International*, *23*(1), 67–77. https://doi.org/10.1080/10106040701538157

Steinemann, A. (2003). DROUGHT INDICATORS AND TRIGGERS: A STOCHASTIC APPROACH TO EVALUATION. *Journal of the American Water Resources Association*, *39*(5), 1217–1233. https://doi.org/10.1111/j.1752-1688.2003.tb03704.x

Thai Meteorological Department. (2015). Annual Weather Summary over Thailand. Retrieved from http://www.tmd.go.th/index.php

Thai Meteorological Department. (2016). Retrieved December 13, 2016, from http://www.tmd.go.th/en/index.php

Thaiturapaisan, T. (2016). Thailand's drought crisis 2016: Understanding it without the panic. Retrieved from https://www.scbeic.com/en/eic_analysis

The US National Drought Mitigation Center. (2016). Retrieved from http://drought.unl.edu/DroughtBasics/TypesofDrought.aspx

Thomas, S. K., & Galbraith, J. M. (2016). *Measuring Saturated Hydraulic Conductivity in Soil*. Virginia state. Retrieved from http://pubs.ext.vt.edu/CSES/CSES-141/CSES-141-PDF.pdf

Thomsen, L. M., Baartman, J. E. M., Barneveld, R. J., Starkloff, T., & Stolte, J. (2015). Soil surface roughness: comparing old and new measuring methods and application in a soil erosion model, *1*, 399–410. https://doi.org/10.5194/soil-1-399-2015

Trimble. (2014). GreenSeeker Handheld | Trimble Agriculture. Retrieved December 6, 2016, from http://www.trimble.com/agriculture/gs-handheld.aspx

Ulaby, F., Batlivala, P., & Dobson, M. (1978). Microwave Backscatter Dependence on Surface Roughness, Soil Moisture, and Soil Texture: Part I-Bare Soil. *IEEE Transactions on Geoscience Electronics*, *16*(4), 286–295. https://doi.org/10.1109/TGE.1978.294586

Ulaby, F., Bradley, G., & Dobson, M. (1979). Microwave Backscatter Dependence on Surface Roughness, Soil Moisture, and Soil Texture: Part II-Vegetation-Covered Soil. *IEEE Transactions on Geoscience Electronics*, *17*(2), 33–40. https://doi.org/10.1109/TGE.1979.294626

USDA. (1951). Soil Survey Manual - Chapter Three | NRCS. Retrieved from https://www.nrcs.usda.gov/wps/portal/nrcs/detail/national/soils/?cid=nrcs142p2_054253

USDA. (2011). *Soil Quality Indicators Soil Electrical Conductivity*.

USGS. (2015). Remote Sensing Phenology. Retrieved January 23, 2017, from https://phenology.cr.usgs.gov/ndvi_foundation.php

Van Reeuwijk, L. (2002). *Procedures for soil analysis (6th edition) | ISRIC World Soil Information*. Wageningen. https://doi.org/90-6672-044-1

Wang, L., & Qu, J. J. (2009). Satellite remote sensing applications for surface soil moisture monitoring: A review. *Frontiers of Earth Science in China*, *3*(2), 237–247. https://doi.org/10.1007/s11707-009-0023-7

Wannakomol, A. (2005). *Soil and Groundwater Salinization Problems in the Khorat Plateau, NE Thailand - Integrated Study of Remote Sensing, Geophysical and Field Data*. *Dissertationen Online*. Freien Universität Berlin. Retrieved from http://www.diss.fu-berlin.de/diss/servlets/MCRFileNodeServlet/FUDISS_derivate_000000001672/02_wannakomolch2.pdf?hosts=

Wardlow, B. D., Anderson, M. C., & Verdin, J. P. (2012). *Remote sensing of drought innovative monitoring approaches* (1st ed.). London: CRC Press.

Warren, J. (1999). *Evaporites : their evolution and economics*. Blackwell Science.

Warrence, N. J., Bauder, J. W., & Pearson, K. E. (2003). *Basics of Salinity and Sodicity Effects on Soil Physical Properties*.

Wilhite, D. A., & Glantz, M. H. (1985a). Understanding: the Drought Phenomenon: The Role of Definitions. *Water International*, *10*(3), 111–120. https://doi.org/10.1080/02508068508686328

Wilhite, D. A., & Glantz, M. H. (1985b). Understanding the Drought Phenomenon: The Role of Definitions. *Water International*, *10*(3), 111–120. Retrieved from http://digitalcommons.unl.edu/droughtfacpub

World Meteorological Organization. (2012). Standardized Precipitation Index User Guide. Retrieved from www.wmo.int/agm

Wu, W., Mhaimeed, A. S., Al-Shafie, W. M., Ziadat, F., Dhehibi, B., Nangia, V., & De Pauw, E. (2014). Mapping soil salinity changes using remote sensing in Central Iraq. *Geoderma Regional*, *2*, 21–31. https://doi.org/10.1016/j.geodrs.2014.09.002

Zargar, A., Sadiq, R., Naser, B., & Khan, F. I. (2011). A review of drought indices. *Environmental Reviews*, *19*(NA), 333–349. https://doi.org/10.1139/a11-013

APPENDIXES

Appendix 1. The calculation of the 3 month SPI for August in Microsoft Excel 2010

Here the 3 month SPI during 1968 – 2016 for August is based on the total rainfall for August, September and October corresponding rice cultivation period.

A. Estimation of gamma distribution parameter α and β for August

	mean	Ln(mean)	U	α	β
August	456.65	6.12	0.059	8.57	53.27

B. The 3 month SPI for August

Year	Total rainfall For August	Ln of Rainfall	Gamma transform	H transform	T transforn	SPI
1986	523.2	6.26	0.70	0.70	1.55	0.52
1987	516	6.25	0.68	0.68	1.52	0.48
1988	433.5	6.07	0.49	0.49	1.15	-0.04
1989	296.3	5.69	0.14	0.14	0.56	-1.04
1990	389.6	5.96	0.37	0.37	0.96	-0.34
2012	243.8	5.50	0.06	0.06	0.36	-1.47
2013	369.9	5.91	0.32	0.32	0.87	-0.48
2014	410.4	6.02	0.42	0.42	1.05	-0.19
2015	432.7	6.07	0.48	0.48	1.15	-0.04
2016	565.6	6.34	0.78	0.78	1.73	0.76